https://doi.org/10.5194/egusphere-2025-1310
Preprint. Discussion started: 28 March 2025

Dense shelf-water and associated sediment transport in the Cap de Creus Canyon and adjacent shelf under mild winter regimes: insights from the 2021-2022 winter

Marta Arjona-Camas [1,2,*], Xavier Durrieu de Madron[2], François Bourrin[2], Helena Fos[1], Anna Sanchez-Vidal[1], David Amblas[1]
[1]GRC Geociències Marines, Departament de Dinàmica de la Terra i de l'Oceà, Universitat de Barcelona, Barcelona, Spain.
[2]CEFREM, UMR-5110 CNRS-Université de Perpignan Via Domitia, Perpignan, France.

Correspondence to: Marta Arjona-Camas (marjona@ub.edu)

Abstract. This study examines dense shelf water cascading (DSWC) and estimates the dense shelf-water and associated sediment transport in the Cap de Creus Canyon (northwestern Mediterranean) during the mild winter of 2021-2022. The FARDWO-CCC1 multiplatform survey in March 2022 revealed dense shelf waters on the continental shelf, which were transported to the canyon head. These cold, dense, and turbid waters, rich in dissolved oxygen and chlorophyll-a, downwelled along the canyon's southern flank to depths around 350 m. During the observed downwelling event, estimated water and suspended sediment transport within the dense water vein were 0.3 Sv and 10^5 metric tons, respectively, mainly confined to upper canyon reaches. These transports were low compared to extreme winters, likely due to the influence of freshwater inputs and moderate meteorological winter conditions. Transport magnitudes were higher in the upper canyon section than in the mid-canyon section, where transport was estimated at 0.05 Sv, including around 10^4 metric tons of sediment. This observation suggests that during mild winters, while most of the dense water either remains on the shelf or the shelf-edge area, or flows southward along the coast, the Cap de Creus Canyon acts only as a partial sink for cascading waters. Mediterranean Sea Physics reanalysis data showed that the cascading season lasted approximately three months, from January to early April 2022, with several cascading pulses within the canyon. The highest dense shelf water transport occurred in mid-March, associated with easterly/south-easterly windstorms. This study confirms that remarkable dense shelf water and sediment transport occurs in the Cap de Creus Canyon, particularly along its southern flank, even during mild winters in absence of deep cascading and limited external forcing. Nevertheless, this phenomenon appears to make a significant contribution to the formation of Western Intermediate Water (WIW) in the region.

Keywords: dense shelf water cascading; Western Intermediate Water; mild winter; sediment transport; Gulf of Lion; Mediterranean Sea.

1 Introduction

Continental margins are crucial transitional areas that link the terrestrial system to the deeper ocean (Nittrouer et al., 2009; Levin and Sibuet, 2012). These regions receive significant inputs of particulate material, mainly of fluvial and atmospheric origin in mid-latitude margins, which accumulate into extensive deposits on the continental shelf (Blair and Aller, 2012; Liu et al., 2016; Kwon et al., 2021). However, these inputs can be reworked and partially exported to deeper areas of the ocean by various hydrodynamic processes (Walsh and Nittrouer, 2009). These processes include river floods that transfer large quantities of suspended sediments to the margin, and high-energy storm waves that resuspend sediment from the shallower regions of the shelf. Both mechanisms can transport elevated amounts of suspended particulate matter (SPM) into deeper areas of the slope, often through submarine canyons, as turbidity currents or hyperpycnal flows (Liu et al., 2012; Puig et al., 2014).

The Gulf of Lion (GoL), in the northwestern Mediterranean, is a very interesting region for the study of shelf-slope exchanges, as it receives important inputs from both rivers and atmospheric deposition (Durrieu de Madron et al., 2008). Moreover, it is a very dynamic area where strong physical forcing prevails and where episodic events, such as storms or dense

https://doi.org/10.5194/egusphere-2025-1310
Preprint. Discussion started: 28 March 2025

shelf water cascading (DSWC), contribute to the efficient export of shelf water and sediment towards the open sea and deeper parts of the basin (Millot, 1990; Canals et al., 2006; Palanques et al., 2006, 2008; Ogston et al., 2008). The formation of dense waters is essentially related to atmospheric forcing and occurs in winter by heat loss and evaporation induced by active and persistent (more than 30 days) northerly and north-westerly winds (locally named Tramontane and Mistral). This results in cooling, vertical mixing, and densification of waters over the GoL's shelf (Durrieu de Madron et al., 2005, 2008; Canals et al., 2006). These dense waters sink until reaching their equilibrium depth and propagate along the western coast of the GoL (Fig. 1). The preferential cyclonic circulation of coastal currents, combined with the narrowing of the shelf at the southwestern end of the gulf, cause most of the export from the shelf mainly through the Lacaze-Duthiers and Cap de Creus canyons (Ulses et al., 2008b; Palanques et al., 2008). There, dense shelf waters overspill and cascade down the slope (Béthoux et al., 2002; Durrieu de Madron et al., 2005), contributing to the ventilation of intermediate and deep waters and altering the geomorphology of the seabed along its path by eroding and depositing sediments. It can also transport organic matter accumulated on the shelf to the slope and basin, and ultimately impact the functioning of deep-sea ecosystems (Bourrin et al., 2006, 2008; Heussner et al., 2006; Sanchez-Vidal et al., 2008).

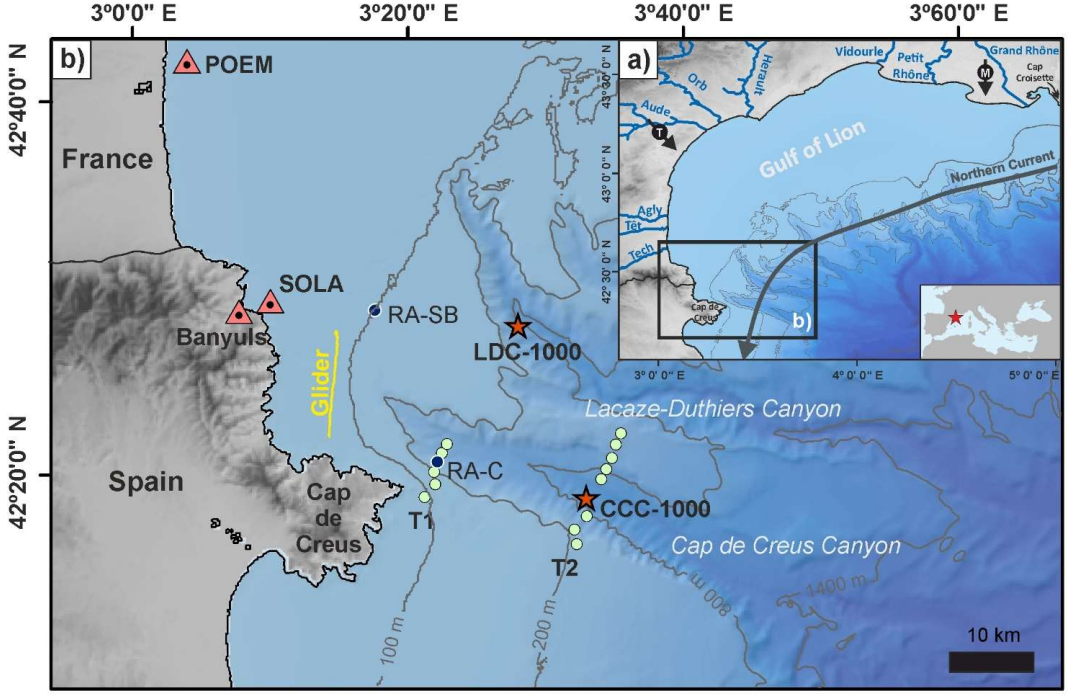

Figure 1. (a) Bathymetric map of the GoL showing the rivers discharging into the gulf and the incised submarine canyons. Black arrows depict Tramontane and Mistral winds. The grey arrow indicates the direction of the Northern Current over the study area. (b) Bathymetric map of the southwestern part of the Gulf of Lion showing the location of Lacaze-Duthiers Canyon (LDC) and Cap de Creus Canyon (CCC). Orange triangles indicate the location of buoys (POEM, Banyuls, and SOLA). The location of the re-analysis grid-points at the shelf break (RA-SB) and within the CCC (RA-C) are indicated with dark blue dots. Green dots represent the location of CTD stations carried out during the FARDWO-CCC1 cruise. Red stars mark the location of two instrumented mooring lines deployed at ~1000 m depth at the axis of LDC (LDC-1000) and CCC (CCC-1000). The solid yellow line indicates the glider section on the continental shelf adjacent to the CCC.

https://doi.org/10.5194/egusphere-2025-1310
Preprint. Discussion started: 28 March 2025

Several studies conducted in the GoL have investigated the importance of extreme DSWC events on shelf-slope exchanges. These particularly intense events were monitored in winters 1998-1999 (Heussner et al., 2006), 2004-2005 (Canals et al., 2006; Ogston et al., 2008; Puig et al., 2008), 2005-2006 (Pasqual et al., 2010; Sanchez-Vidal et al., 2008), and 2011-2012 (Durrieu de Madron et al., 2013; Palanques and Puig, 2018) by instrumented mooring lines placed at depths ~1,000 m in Lacaze-Duthiers and Cap de Creus Canyons. One of the most studied extreme events is the DSWC that occurred in the severe winter of 2004-2005. Over 40 days, more than two thirds (750 km^3) of GoL's shelf waters cascaded through the Cap de Creus Canyon (Canals et al., 2006; Ulses et al., 2008b), maintaining cold temperatures (11-12.7 ºC), high down-canyon velocities (> 0.8 $m \cdot s^{-1}$) and high suspended sediment concentrations (30-40 $mg \cdot L^{-1}$). This DSWC event also transported ~$0.6 \cdot 10^6$ tons of organic carbon downcanyon, a mass comparable to the mean annual solid transport of all rivers discharging into the GoL (Canals et al., 2006; Tesi et al., 2010).

Nonetheless, moderate DSWC events are the most common since the set of the observational era in the GoL, and they are expected to become even more prevalent under the climate change scenario (Herrmann et al., 2008; Durrieu de Madron et al., 2023). These events typically occur during mild winters, driven by quieter atmospheric conditions and lower heat losses (Martín et al., 2013; Rumín-Caparrós et al., 2013; Mikolajczak et al., 2020). During such winters, intense cold continental winds, which are key for dense water formation, are less frequent than usual (less than 30 days) and rarely exceed speeds of 10 $m \cdot s^{-1}$. In contrast, easterly and southeasterly winds are unusually frequent and often blow for more than three consecutive days (Mikolajczak et al., 2020). Additionally, moderate to high river discharges, particularly from the Rhône River, further limit the densification of shelf waters (Ulses et al., 2008a). As a result of these forcings, the density of shelf waters remains moderate, with less buoyancy loss than in extreme events (Mikolajczak et al., 2020). Consequently, dense waters over the GoL's shelf are mainly consumed by mixing with lighter ambient waters, and only a small fraction of them escapes to deeper areas of the slope (Herrmann et al., 2008). For instance, during the mild winter of 2003-2004, Ulses et al. (2008a) estimated a total export of dense shelf waters of 75 km^3, an order of magnitude smaller than during extreme events. Another good example is the winter of 2010-2011, when only brief and shallow cascading was recorded (Martín et al., 2013; Rumín-Caparrós et al., 2013). In March 2011, the CASCADE experiment monitored the hydrodynamics of the upper sector of the Cap de Creus Canyon during a period of low loss of buoyancy (Martín et al., 2013; Bourrin et al., 2015), capturing the downwelling of cold, low salinity, and turbid waters to 350 m depth on the canyon's southern flank (Martín et al., 2013). Numerical simulations by Mikolajczak et al. (2020) indicate that, despite contrasting atmospheric conditions, the total dense water export during the mild winter of 2010-2011 (1,500 km^3) was of the same magnitude as during the extreme winter of 2004-2005 (1,640 km^3) (Ulses et al., 2008a). The key difference lay in the preferential export pathways: in winter 2010-2011, 30 % of the export occurred through the Cap de Creus Canyon, while 70 % followed along the coast. This distribution was reversed in winter 2004-2005, when 69 % of the exported dense shelf water passed through the canyon (Ulses et al., 2008a). However, the limited number of observations in the Cap de Creus Canyon during the mild winter of 2010-2011, mainly based on moored time series, constrained the full characterization of the shelf-to-canyon export of dense shelf waters during this moderate DSWC event.

The present study aims to comprehensively investigate the hydrographic characteristics, hydrodynamics and export routes of a mild cascading event in the Cap de Creus Canyon and its adjacent shelf during the winter of 2021-2022. This work is based on hydrographic data collected during a multiplatform survey in the Cap de Creus Canyon, which was monitored during the FARDWO-CCC1 cruise, and simultaneous measurements at its adjacent shelf acquired during a glider survey as part of the MELANGE-DUNES experiment. These datasets enabled us to capture the dynamics of the event over two days in March 2022 and directly quantify the export of water and suspended particulate matter. To provide a broader temporal perspective, reanalysis data were used to determine the duration of the cascading season and estimate the variability of dense shelf water export within the Cap de Creus Canyon during the mild winter of 2021-2022.

https://doi.org/10.5194/egusphere-2025-1310
Preprint. Discussion started: 28 March 2025

2 Study area

2.1 General setting

The GoL is a micro-tidal river-dominated continental margin that extends from the Cap Croisette Peninsula, in the northern part of the gulf, to the Cap de Creus Peninsula at its southwestern limit (Fig. 1a). It is characterized by a wide continental shelf (up to 70 km) and it is incised by a dense network of submarine canyons (Lastras et al., 2007).

The ocean circulation of the GoL is primarily driven by the Northern Current, which flows along the continental slope from the northeast to the southwest (Millot, 1990; Raimbault et al., 2003). This current is part of the cyclonic general circulation of the Western Mediterranean basin and it is especially intense during winter months (Lapouyade and Durrieu de Madron, 2001; Petrenko et al., 2008). The GoL is also impacted by strong continental winds from the north and northwest (Mistral and Tramontane, respectively), which favor dense water formation and cascading events in winter (Durrieu de Madron et al., 2013) and coastal upwellings in summer (Odic et al., 2022). Humid easterly and southeasterly winds, which blow less frequently, occur primarily from autumn to spring, and can produce large swells and high waves over the continental shelf (Ferré et al., 2005; Leredde et al., 2007; Petrenko et al., 2008; Guizien, 2009). They do not produce a densification of surface waters but lead to an intense cyclonic circulation on the GoL's shelf and to a strong export at the southwestern exit of the Gulf (Ulses et al., 2008a; Mikolajczak et al., 2020). The ocean circulation of the GoL is also influenced by the freshwater inputs from the Rhône River, one of the largest Mediterranean Rivers, and a series of smaller rivers with typical flash-flooding regimes (Ludwig et al., 2009). The Rhône River supplies an annual river discharge of 1,700 $m^3 \cdot s^{-1}$ and an average of 8.4 $Mt \cdot y^1$ of suspended particulate matter (Sadaoui et al., z2016; Poulier et al., 2019). The smaller rivers (from south to north the Tech, Têt, Agly, Aude, Orb, Hérault, Lez, and Vidourle) account for slightly 5% of the total inputs of particulate matter (~0.5 $Mt \cdot y^{-1}$) to the GoL (Serrat et al., 2001; Bourrin et al., 2006). Most of the sediment delivered by these rivers is temporarily stored near their mouths in deltas and prodeltas (Drexler and Nittrouer, 2008), and afterwards it is remobilized and redistributed along the margin by the action of storms and the permanent Northern Current (Millot, 1990; Guillén et al., 2006; Ulses et al., 2008a; Estournel et al., 2023). This westerly current carries particulate material from the shelf towards the southwestern end of the GoL, where the continental shelf rapidly narrows and the Cap de Creus Peninsula acts as a barrier to the flow, increasing the concentration of water and particles (Durrieu de Madron et al., 1990; Canals et al., 2006).

The Cap de Creus Canyon represents the limit between the GoL and the Catalan margin (Fig. 1b). The canyon head is located only 4 km from the coast and incises the shelf edge at 110-130 m depth (Lastras et al., 2007). Due to its proximity to the coast and the preferential direction of coastal currents, this canyon has been identified as the main pathway for the transfer of water and sediments from the shelf to the slope and deep margin (Canals et al., 2006; Palanques et al., 2006, 2012).

2.2 Hydrography

The surface layers in the GoL stratify between late spring and autumn (Millot, 1990). In winter, the stratification weakens due to the cold temperatures, and the water column becomes homogeneous (Durrieu de Madron and Panouse, 1996). Offshore, the GoL is characterized by several water masses. The Atlantic Water (AW) fills the upper 250 m and flows into the Mediterranean Sea through the Strait of Gibraltar. During its transit to the GoL, its hydrographic properties undergo chemical and physical modifications, becoming the "old" Atlantic Water (oAW) with T > 13 ºC and S = 38.0-38.2 (Millot, 1999). Below, the Eastern Intermediate Water (EIW) occupies the water column between 250 and 850 m depth. It is formed during winter in the Levantine Basin, in the Eastern Mediterranean Sea, by intermediate convection (Font, 1987; Millot, 1999; Taillandier et al., 2022; Schroeder et al., 2024). The Western Mediterranean Deep Water (WMDW) occupies the deepest bathymetric levels and is formed in winter at interannual scales in the GoL by open-ocean deep convection. It typically shows T ~ 13 ºC and S = 38.43-38.47 (Marshall and Schott, 1999; Somot et al., 2016). During winter, Mistral and Tramontane winds cause the formation of dense shelf waters (DSW) over the GoL (T < 13 ºC and S < 38.4) (Houpert et al., 2016; Testor et al., 2018). DSW can be

https://doi.org/10.5194/egusphere-2025-1310
Preprint. Discussion started: 28 March 2025

detached at intermediate depths and contribute to the Western Intermediate Water (WIW) (T = 12.6-13.0 ºC and S = 38.1-38.3) body, which is found at upper slope depths (~350 m) (Dufau-Julliand et al., 2004; Durrieu de Madron et al., 2005; Juza et al., 2013). This occasionally happens in autumn or during mild winters, when the downwelling of DSW is limited to 300-400 m depth by stratification. The formation of WIW is an important process in the Mediterranean thermohaline circulation, as it contributes to the ventilation of intermediate layers and plays a role in preconditioning the region for deeper convection events. During the coldest winters, the excess density gains allows DSW to reach the deep basin around 2000-2500 m depth, and contributes to the ventilation of the deep waters and to the final characteristics of the WMDW (Durrieu de Madron, 2013; Palanques and Puig, 2018).

3 Materials and methods

3.1 Field data acquisition

3.1.1 Hydrographic transects and current vertical profiles

During the FARDWO-CCC1 Cruise, onboard the R/V *García del Cid*, two hydrographic transects were conducted on March 5-6, 2022, across the Cap de Creus Canyon, with stations spaced every 1.5 km (Fig. 1b). The T1 transect covered the upper section of the canyon, while the T2 transect covered the mid-canyon section. The hydrographic data were collected using a SeaBird 9 CTD probe coupled with a SeaPoint Fluorometer and Turbidity Sensor (700 nm), an SBE43 dissolved oxygen sensor, and a WetLabs C-Star Transmissometer (650 nm). These sensors were mounted on a rosette system with twelve 12 L Niskin bottles, which collected water samples from various depths. The CTD-Rosette system was hauled through the water column, allowing the comparison of sensor outputs in productive surface waters with high fluorescence, in clear mid-waters, and in intermediate and bottom nepheloid layers loaded with fine suspended particulate matter. Potential temperature, practical salinity, and potential density were calculated using the state of the seawater TEOS-10 equation (Feistel, 2003; 2008).

Velocity profiles were simultaneously measured using two Lowered Acoustic Doppler Current Profiler (LADCPs) Teledyne 300 kHz narrowband units mounted on the CTD frame. One unit faced upwards and the other downwards to maximize the total range of velocity observations. Each instrument was configured with 20 bins, each 8 m in length, which allowed for a measurement range of ~160 m (Thurnherr, 2010). The raw LADCP data were processed using the LDEO Software version IX by applying the least-squared method, using the navigation and the vessel-mounted (VM) ADCP data as constraints (Visbeck, 2002).

3.1.2 Vessel-mounted (VM) ADCP data

The R/V *García del Cid* was equipped with a vessel-mounted (VM) 75 kHz ADCP (Ocean Surveyor, RD Instruments) that recorded current velocities along the hydrographic sections. The VM-ADCP was configured to record current velocities at 2-min averages, while sampling depths were set to 8-m vertical bins. The VM-ADCP data were processed using the CASCADE V7.2 software (Le Bot et al., 2011). Absolute current velocities resulted from removing the vessel speed, derived from a differential global positioning system. The measurement range of the instrument was from 20 m to 720 m depth. Given the micro-tidal regime of the Mediterranean Sea (tidal range ~ 0.5 m), tides are considered of very low magnitude in the GoL (Davis and Hayes, 1984; Dipper, 2022). Nevertheless, a barotropic tide correction was applied to the VM-ADCP data using the OTIS-TPX8 Tide model (https://www.tpxo.net/global) within the cascade V7.2 software, which provided tide-corrected current velocities. VM-ADCP data were then screened to align with the timeframe of the different hydrographic sections. However, the VM-ADCP's range could not fully cover the water column due to the interaction of secondary acoustical lobes with the seabed. To address this limitation, we integrated VM-ADCP data with LADCP measurements recorded at each station. This integration involved aligning time stamps, matching coordinate systems, and merging and interpolating datasets.

https://doi.org/10.5194/egusphere-2025-1310
Preprint. Discussion started: 28 March 2025

Finally, ADCP velocities, decomposed into E-W and N-S components, were rotated 15º counterclockwise to align with the local canyon axis orientation. This rotation provided the across- and along-canyon velocity components for interpretation. For the across-canyon component, eastward velocities have been defined as positive and westward velocities as negative. For the along-canyon component, up-canyon velocities are positive, while down-canyon velocities are negative.

3.1.3 Glider observations

The hydrodynamics of dense shelf waters at the southwestern tip of the continental shelf adjacent to the Cap de Creus Canyon were monitored by a SeaExplorer underwater glider (ALSEAMAR-ALCEN). The glider carried out one along-shelf (i.e., north-south) section and navigated 10 km for 25 hours, starting on March 5, 2022 (Fig. 1b). It conducted a total of 28 yos (down/up casts). It followed a sawtooth-shaped trajectory through the water column, descending typically to 2 m above the bottom and ascending to 0-1 m of distance from the surface. The glider was equipped with a pumped SeaBird GPCTD, coupled with a dissolved oxygen sensor (SBE43F), that acquired temperature, conductivity, and pressure data at a sampling rate of 4s. Salinity, potential temperature, and potential density were derived using the TEOS-10 equation (Feistel, 2003; 2008). Additionally, the glider had a SeaBird Triplet (WetLabs FLBBCD sensor), which measured proxies of phytoplankton abundance (by measuring the fluorescence of chlorophyll-a at 470/695 nm), and total particle concentration (by measuring optical backscattering at 700 nm). Finally, the glider integrated a downward-looking AD2CP (Acoustic Doppler Dual Current Profiler) that measured relative water column velocities and the glider speed. The AD2CP was configured with 15 vertically stacked cells of 2 m resolution, and a sampling frequency of 5 s. Raw velocity measurements were processed using the shear method to derive absolute current velocities (Fischer and Visbeck, 1993; Thurnherr et al., 2015; Homrani et al., 2025). We used bottom tracking and GPS coordinates as constraints to reference each velocity profile.

3.2 Ancillary data

3.2.1 Monitoring of dense shelf waters

The SOLA station, located in the Bay of Banyuls-sur-Mer (42.48º N and 3.13º E) and managed by the SOMLIT (https://www.seanoe.org/data/00886/99794/; Conan et al., 2024), was used to monitor the presence of dense shelf waters at the continental shelf during winter 2021-2022 (Fig. 1b). This station provided weekly near-bottom (~27 m depth) time series data on temperature, salinity, and pressure. Raw data were processed to remove gaps and outliers.

The Mediterranean Sea Physics Reanalysis (hereafter MedSea) was used to evaluate the temporal evolution of dense shelf waters at the shelf break and the Cap de Creus Canyon during the same period. The model has an horizontal grid resolution of 1/24º (approximately 4-5 km). Temperature and salinity were extracted from two grid points along the path of the along-slope current: one at the shelf break (RA-SB: 42.48 °N and 3.29 °E, depth = 250 m) and another within the Cap de Creus Canyon (RA-C: 42.34 °N and 3.37 °E, depth = 350 m) (Fig. 1b).

3.2.2 Meteorological and wave data, and river discharge

Heat flux data were used to evaluate the interaction between the atmosphere and the ocean surface. Data was retrieved from the European Centre for Middle-range Forecast (ECMWF) ERA5 reanalysis by Copernicus Climate Change Service. This global reanalysis product provides hourly estimates of a large number of atmospheric variables since 1940, with a horizontal resolution of 0.25 º (Hersbach et al., 2023). For this study, the sea-atmosphere interactions were assessed from 42.6 °N to 43.4 °N and from 3 °E to 4.5 °E, approximately covering the entire GoL's continental shelf, from July 2021 to July 2022.

Significant wave height (Hs) data were retrieved from the Banyuls buoy (06601) located at 42.49 °N and 3.17 °E (Fig. 1b), through the French CANDHIS database (https://candhis.cerema.fr). These measurements were recorded every 30 min using a directional wave buoy (Datawell DWR MkIII 70). Wind speed and direction data were obtained from the POEM

https://doi.org/10.5194/egusphere-2025-1310
Preprint. Discussion started: 28 March 2025

buoy (https://www.seanoe.org/data/00777/88936/; Bourrin et al., 2022), which records hourly observations using a surface meteorological sensor.

Water discharge from rivers opening to the GoL was retrieved from Hydro Portail v3.1.4.3 (https://hydro.eaufrance.fr). For this study, we have considered the river discharge from the Rhône River and the total discharge from coastal rivers as the sum of their individual contribution.

3.2.3 Instrumented mooring lines

Current velocity and direction, temperature, and SPM concentration were monitored in two submarine canyons, the Lacaze-Duthiers and the Cap de Creus canyons, by means of two instrumented mooring lines (Fig. 1b). The mooring line at Lacaze-Duthiers Canyon, located at about 1000 m depth, has been maintained in the canyon since 1993 as part of the MOOSE program. It is equipped with two current meters (Nortek Aquadopp 2 MHz) with temperature, conductivity, and turbidity sensors, placed at 500 m and 1,000 m depth (referred to as LDC-500 and LDC-1000, respectively). The sampling interval for the current meters was set to 60 min. The fixed mooring line at the Cap de Creus Canyon has been maintained in the canyon axis by the University of Barcelona since 2009. This mooring line, referred to as CCC-1000, is equipped with a current metter (Nortek Aquadopp 2 MHz) with temperature, conductivity, and a SeaPoint turbidity sensors placed at 18 m above the bottom (mab). The current meter sampling interval was set to 15 min. For this study, the recording period was considered from October 2021 to April 2022, which encompassed the winter period and the FARDWO-CCC1 Cruise.

3.3 Determination of suspended particulate matter (SPM) concentration from turbidity measurements

To calibrate turbidity measurements obtained in the Cap de Creus Canyon during the FARDWO-CCC1 Cruise, water samples were collected at selected depths with Niskin bottles. For each sample, between 2 and 3 L of water were vacuum filtered into 47 mm 0.4 µm pre-weighted Nucleopore filters. The filters were then rinsed with MiliQ water to remove salt and stored at 4 ºC. Then, these filters were dried by desiccation and weighted. The weighing difference of the filters divided by the volume filtered of seawater yielded to the SPM concentration, in $mg \cdot L^{-1}$. Finally, the measured SPM concentrations were plotted against in situ turbidity measurements, both from the transmissometer and the optical sensor (Figs. 2a, b). The beam attenuation coefficient (BAC) from the transmissometer showed a stronger correlation with SPM ($R^2 = 0.86$) compared to FTU from the SeaPoint turbidity sensor ($R^2 = 0.81$). Therefore, SPM concentrations were predicted using the equation:

$$SPM = 1.84 \cdot BAC + 0.05 \ (R^2 = 0.85;\ n = 25) \quad (1)$$

https://doi.org/10.5194/egusphere-2025-1310
Preprint. Discussion started: 28 March 2025

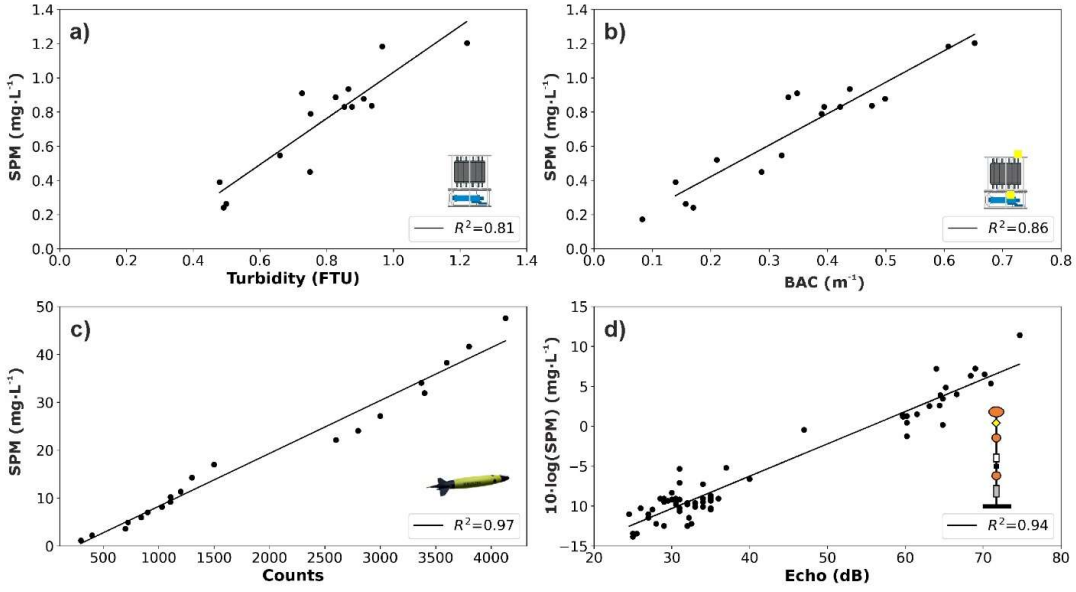

Figure 2. Relationship between the weighed SPM mass concentration (mg·L^{-1}) and: (a) turbidity records (FTU) from the SeaPoint sensor and (b) BAC (m^{-1}) from the WetLabs transmissometer attached to the CTD-rosette system; (c) optical backscatter sensor data (counts) from the WetLabs FLBBCD sensor mounted on the SeaExplorer glider; (d) echo intensity (dB) retrieved from the current meters installed in LDC and CCC instrumented moorings. For each relationship, the regression coefficient (R^2) is given.

Backscatter data (in counts) from the optical sensor on the SeaExplorer glider were also correlated to SPM concentration using a laboratory calibration. Firstly, the optical sensor was submerged into a 10-L plastic tank filled with freshwater. Then, sediment was added while stirring the water to distribute the sediment particles evenly. The amount of sediment was gradually increased until the instrument reached a saturation level of approximately 4,000 counts, corresponding to a sediment mass of 447.5 mg. The optical sensor, connected to a computer, displayed and stored the turbidity measurements during the calibration process. Then, water samples were taken at each interval and filtered, obtaining SPM concentration (in mg·L^{-1}). Pairs of counts/SPM data points yielded the following regression line (Fig. 2c):

$$SPM = 0.01 \cdot counts \ (R^2 = 0.97;\ n = 20) \quad (2)$$

Finally, echo intensity (EI) records from the current meters equipped in LDC and CCC lines were also correlated with SPM concentration, using a linear equation relating the logarithm of SPM to EI (Gartner, 2004). Unlike optical devices, acoustic sensors measure relative particle concentrations based on changes on the backscattered acoustic signal (Fugate and Friedrichs, 2002). Acoustic backscatter, expressed in counts, is proportional to the decibel sound pressure level (Lohrmann, 2001), and depends on the particle size and on the operating frequency of the acoustic sensor (Wilson and Hay, 2015). The equation derived from the regression between backscatter data and direct sampling concentration in the GoL was (Fig. 2d):

$$10 \cdot \log (SPM) = 0.405 \cdot EI - 22.46 \ (R^2 = 0.94;\ n = 66) \quad (3)$$

https://doi.org/10.5194/egusphere-2025-1310
Preprint. Discussion started: 28 March 2025

4 Results

4.1 Meteorological and oceanographic conditions during winter 2021-2022

The time series of net heat fluxes from the GoL's shelf showed positive values from July to October 2021 (Fig. 3a). From October 2021 to late March 2022, net heat fluxes progressively decreased to negative values, reflecting a heat loss from the ocean to the atmosphere (Fig. 3a). The strongest net heat losses during that winter occurred in November 2021 and January 2022, reaching values of about -400 $W \cdot m^{-2}$ (Fig. 3a).

Winter 2021-2022 was characterized by frequent northerly and northwesterly winds (Tramontane and Mistral) with speeds ranging from 5 to 18 $m \cdot s^{-1}$ (Fig. 3b). The duration of these wind events varied throughout winter, blowing in short periods of 1 to 3 days during October and December, and in longer periods of 5 to 7 consecutive days during November and February (Fig. 3b). The highest wind speeds during this period exceeded 20 $m \cdot s^{-1}$ and were associated with strong heat losses (Figs. 3b, c). From March to July 2022, the wind pattern alternated between northerly/north-westerly winds and short periods (2-4 days) of easterly/southeasterly winds (Fig. 3b). As in winter, the strongest heat losses, which occurred in April 2022, coincided with a relatively longer period (5 days) of northerly/northwesterly winds with relatively high speeds (> 20 $m \cdot s^{-1}$) (Figs. 3a, b).

Significant wave height (Hs) was generally low during winter, ranging between 0.5 and 2.0 m (Fig. 3c). During this period, a single storm, defined as sustained Hs > 2 m for more than 6 hours (Mendoza and Jimenez, 2009), was recorded on March 13, 2022. This storm was caused by a moderate easterly/south-easterly wind event and was accompanied with Hs > 3 m for more than 20 hours (Fig. 3c).

The mean water discharge of the Rhône River generally displayed average values of about 1,700 $m^3 \cdot s^{-1}$ (Fig. 3d; Pont et al., 2002). However, the discharge exceeded 2,000 $m^3 \cdot s^{-1}$ during early October, early November, and mid-December 2021 (Fig. 3d). A peak of over 5,000 $m^3 \cdot s^{-1}$ occurred in late December, without any associated major storm event (Fig. 3c). Coastal river discharges remained relatively low during all the time period, typically below 200 $m^3 \cdot s^{-1}$, except for a few brief episodes where river discharge reached > 400 $m^3 \cdot s^{-1}$ (Fig. 3d). The highest coastal river discharge occurred on March 13, 2022, concomitantly to an easterly/southeasterly wind event (Fig. 3c). The discharge reached 2,265 $m^3 \cdot s^{-1}$, surpassing the discharge of the Rhône River, which was relatively small (884 $m^3 \cdot s^{-1}$) (Fig. 3d).

The near-bottom temperature time series on the continental shelf, extracted from the POEM buoy, showed a gradual decline from 20 ºC in October 2021 to 13 ºC in March 2022 (Fig. 3e). Salinity fluctuated between 37.8 to 38.1 during the same period, occasionally dropping below 37.8 in parallel with temperature decreases (Fig. 3f). At the shelf break (250 m depth), near-bottom temperature remained constant around 14.5 ºC, except for an increase to 15.5 ºC throughout November and a subsequent decrease below 13 ºC from January to late March 2022 (Fig. 3e). Salinity at the shelf break also remained constant (~38.55) throughout the studied winter (Fig. 3f). At the Cap de Creus Canyon (350 m depth), temperature and salinity remained constant around 14.5 ºC and 38.8, respectively, during winter. However, from late January to late March 2022, both variables occasionally dropped in short-lived pulses to 12.9 ºC and 38.1, respectively, before returning to their previous values (Figs. 3e, f). The potential density anomaly at the shelf and shelf break followed the seasonal temperature variations, and it only increased during February-March 2022 when it peaked at ~28.9 $kg \cdot m^{-3}$ (Fig. 3g). In contrast, density at the Cap de Creus Canyon remained relatively stable throughout the study period, slightly varying between 28.75 and 28.95 $kg \cdot m^{-3}$ (Fig. 3g).

https://doi.org/10.5194/egusphere-2025-1310
Preprint. Discussion started: 28 March 2025

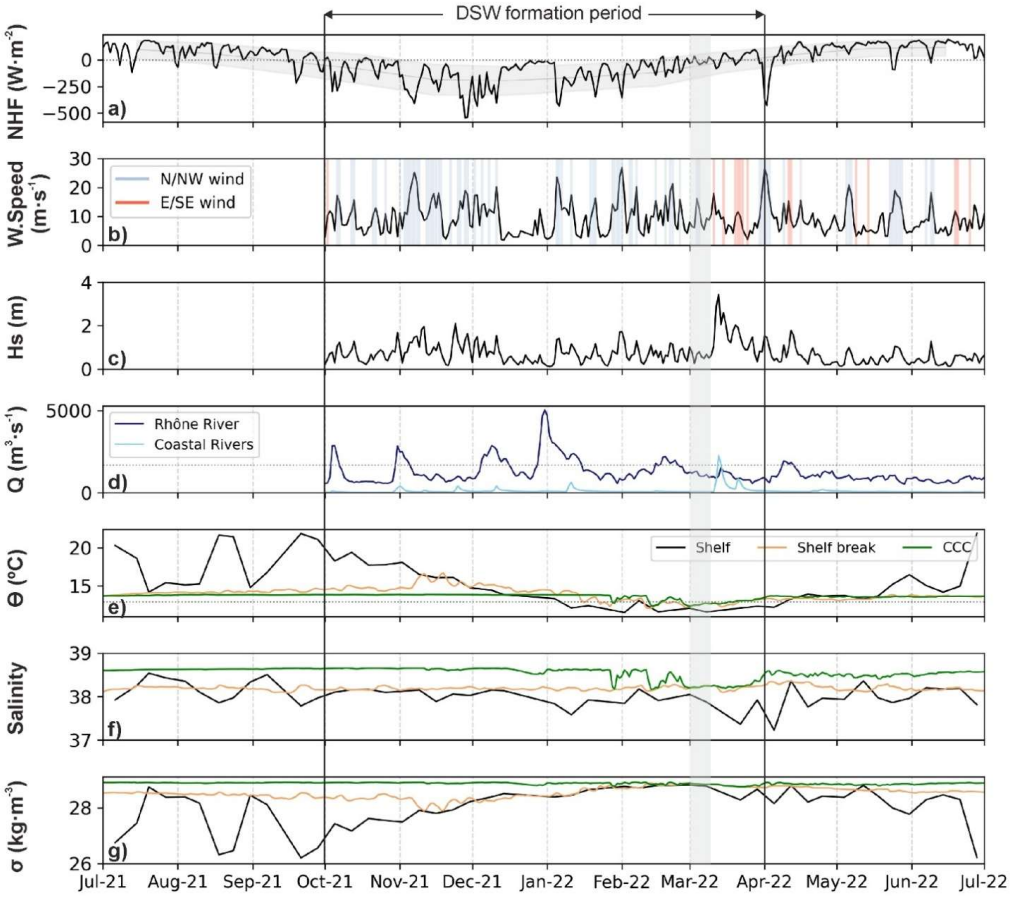

Figure 3. Time series of (a) net heat fluxes (NHF, W·m^{-2}) averaged over the GoL's shelf; (b) wind speed (m·s^{-1}) measured at the POEM buoy. Blue and red shaded bars indicate N/NW and S/SE winds, respectively; (c) significant wave height (Hs, m) measured at the Banyuls buoy; (d) river discharge (Q, m^3·s^{-1}) of the Rhône River (dark blue) and coastal river discharges discharging into the GoL (light blue); (e) weekly mean bottom temperature (Θ, ºC), (f) salinity, and (g) potential density (σ, kg·m^{-3}) calculated from *TS* data at the continental shelf (black), the shelf break (orange), and the Cap de Creus Canyon (green). Data at the continental shelf were extracted from the POEM buoy. Data at the shelf break and within the Cap de Creus Canyon were extracted from two grid points from the Mediterranean Sea Physics Reanalysis product. All data are displayed for the period between July 2021 and July 2022. The grey shaded vertical bar highlights the FARDWO-CCC1 Cruise, which took place on March 1-7th, 2022. The DSW formation period is marked in the figure and corresponds to the period when NHF are negative, indicating ocean heat loss to the atmosphere and enhanced DSWC.

4.2 Time series at LDC and CCC during winter 2021-2022

Time series of temperature, current speed and direction, and SPM concentration at LDC-500, LDC-1000, and CCC-1000 mooring stations during winter 2021-2022 are shown in Figure 4.

https://doi.org/10.5194/egusphere-2025-1310
Preprint. Discussion started: 28 March 2025

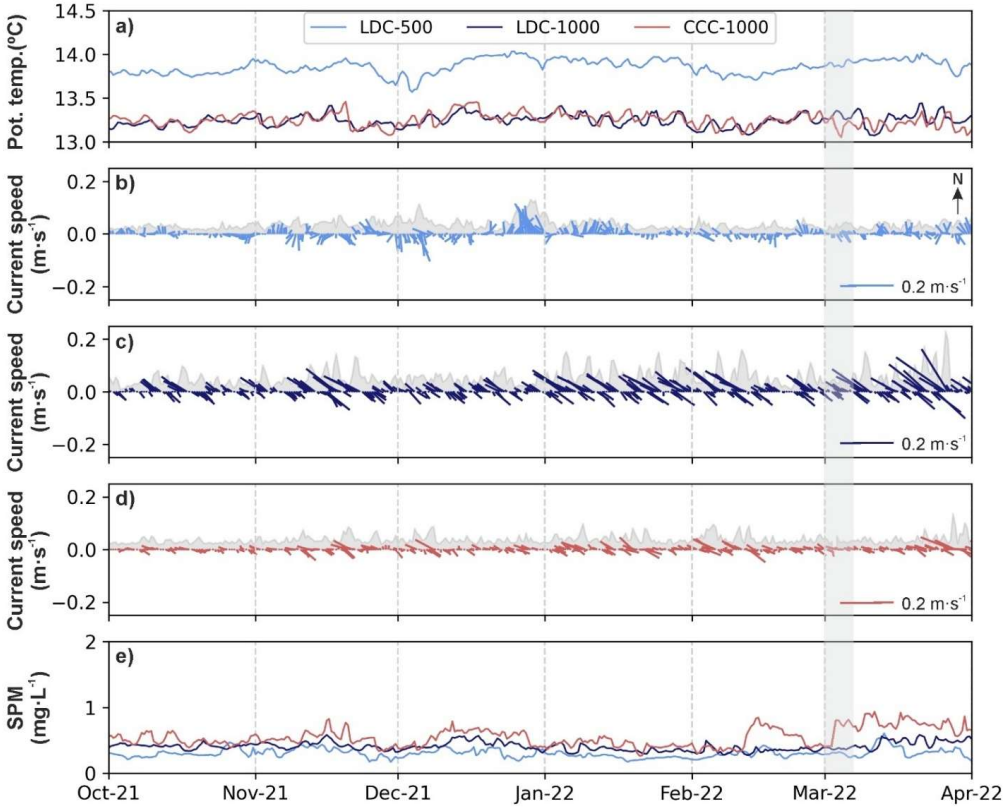

Figure 4. Time series of (a) potential temperature (ºC), (b-d) stick plots of currents and current speed as a shaded grey area ($m \cdot s^{-1}$), and (e) suspended particulate matter concentration (SPM, $mg \cdot L^{-1}$) measured at LDC-500 (light blue), LDC-1000 (dark blue), and CCC-1000 (red) mooring stations. In panels (b-d), arrows indicate the along-canyon component for each mooring site. The grey shaded vertical bar highlights the FARDWO-CCC1 Cruise, which took place on March 1-7, 2022.

At LDC-500, temperature remained relatively constant between 13.5 and 14 ºC, whereas at LDC-1000 and CCC-1000, it fluctuated between 13.1 and 13.4 ºC (Fig. 4a). Current speed was generally low and ranged from 0.01 to 0.1 $m \cdot s^{-1}$ at LDC-500 and CCC-1000 (Figs. 4b, d), and slightly higher at LDC-1000, where it varied between 0.1 and 0.2 $m \cdot s^{-1}$ (Fig. 4c). At LDC-1000, current speed increased several times to 0.12 $m \cdot s^{-1}$ between January and mid-March 2022, and to 0.2 $m \cdot s^{-1}$ in late March (Fig. 4c). A similar, but less intense peak in late March was observed at CCC-1000 (Fig. 4c). These increases coincided with small temperature decreases (Fig. 4a). Current direction at LDC-500 was isotropic (Fig. 4b), whereas at LDC-1000 and CCC-1000 it was anisotropic, aligning preferentially with the axes of Lacaze-Duthiers and Cap de Creus canyons (Figs. 4c, d).

The time series of SPM concentration at all mooring sites showed low values during winter 2021-2022, ranging between 0.2 and 0.5 $mg \cdot L^{-1}$ at all monitored depths (Fig. 4e). The highest SPM concentrations were recorded from mid-February to late March 2022 at CCC-1000, reaching values of > 0.5 $mg \cdot L^{-1}$ (Fig. 4e).

https://doi.org/10.5194/egusphere-2025-1310
Preprint. Discussion started: 28 March 2025

4.3 Water column properties at the CCC and adjacent shelf during the FARDWO-CCC1 Cruise

4.3.1 Hydrographic and biogeochemical properties

The SeaExplorer glider monitored the continental shelf from the surface down to a depth of 92 m at the southwestern tip of the Cap de Creus Canyon. In the northern part of the shelf transect, a water mass with temperatures of 12.9 ºC and salinities of 38.2 occupied most of the water column above the 28.95 $kg \cdot m^{-3}$ isopycnal (Figs. 5a-c). This water mass exhibited SPM concentrations of 1.5-3.0 $mg \cdot L^{-1}$ and dissolved oxygen values of ~232 $\mu mol \cdot kg^{-1}$ (Figs. 6a, c). Near the bottom, a relatively cooler, fresher, and more turbid water mass with higher dissolved oxygen concentrations was observed in the northern part of the section (Figs. 5a-c and 6a-c). This water mass flowed southward along the shelf below the 28.95 $kg \cdot m^{-3}$ isopycnal, gradually becoming slightly warmer, saltier, less turbid, and less oxygenated towards the southern part of the shelf transect (Figs. 5a-c and 6a-c). Fluorescence values generally increased towards the southern part of the shelf transect (Fig. 6b). These hydrographic and biogeochemical properties clearly indicate the presence of dense shelf waters on the continental shelf in the shape of a wedge that thickened towards the coast (i.e., south) near the bottom (Figs. 5a-c and 6a-c).

The FARDWO-CCC1 T1 Transect was carried out across the upper section of the Cap de Creus Canyon, from the surface to a maximum depth of 625 m. The upper water column (< 100 m depth) was characterized by temperatures of 13-13.2 ºC, salinities of ~38.25 (Figs. 5d, e), dissolved oxygen concentrations of ~200 $\mu mol \cdot kg^{-1}$, and relatively low SPM concentrations (0.3 $mg \cdot L^{-1}$) (Figs. 6d, f). Beneath this layer, a colder (12.2-12.7 ºC), fresher (S = 38.1-38.2) water mass occupied depths of 100-350 m along the southern flank of the canyon (Fig. 5d, f). This water mass showed relatively high dissolved oxygen values (> 200 $\mu mol \cdot kg^{-1}$) and increased SPM concentrations (1-1.2 $mg \cdot L^{-1}$) (Figs. 6d-f). It extended ~3 km into the canyon interior. Fluorescence values were generally high (0.5-1.1 $\mu g \cdot L^{-1}$) in the upper 400 m of the water column (Fig. 6e). Below, a relatively cooler, saltier, less oxygenated, and slightly denser (~29.55 $kg \cdot m^{-3}$) water mass was apparent around 350-400 m depth (Figs. 5d-f). Deeper into the canyon (> 400 m depth), a much warmer (T > 13 ºC) and saltier (S ~ 38.4) water mass with lower SPM concentrations and fluorescence values was observed (Figs. 5d-f and 6d-f).

Further offshore, the T2 transect crossed the middle sections of the Cap de Creus Canyon and covered the entire water column down to a depth of 850 m (Figs. 5g-i and 6g-i). The upper 250 m showed a remarkably homogeneous water mass throughout the canyon. It was characterized by temperatures of 13.2-13.4 ºC, salinities of ~38.2, relatively high dissolved oxygen values (197 $\mu mol \cdot kg^{-1}$), and low SPM concentrations (0.3 $mg \cdot L^{-1}$) (Figs. 5g-i and 6g-i). Below this layer, and down to 380 m depth, a much colder (12.2-12.3 ºC), fresher (38.1), highly oxygenated (200-203 $\mu mol \cdot kg^{-1}$) and moderately turbid (0.8-1.0 $mg \cdot L^{-1}$) water mass was observed (Figs. 5g-i and 6g-i). This water mass only occupied the southern flank of the canyon and extended approximately 2.5 km into the interior of the canyon (Figs. 5g-i and 6g-i). Fluorescence values ranged from 0.18 to 0.60 $\mu g \cdot L^{-1}$ throughout the canyon from the surface to ~380 m depth above the 29.0 $kg \cdot m^{-3}$ isopycnal (Fig. 6h). Finally, between 400 m and 850 m depth, the water column was characterized by temperatures of ~13.1 ºC, salinities of 38.4, and relatively low oxygen concentrations, fluorescence values, and SPM concentration (Figs. 6g-i).

https://doi.org/10.5194/egusphere-2025-1310
Preprint. Discussion started: 28 March 2025

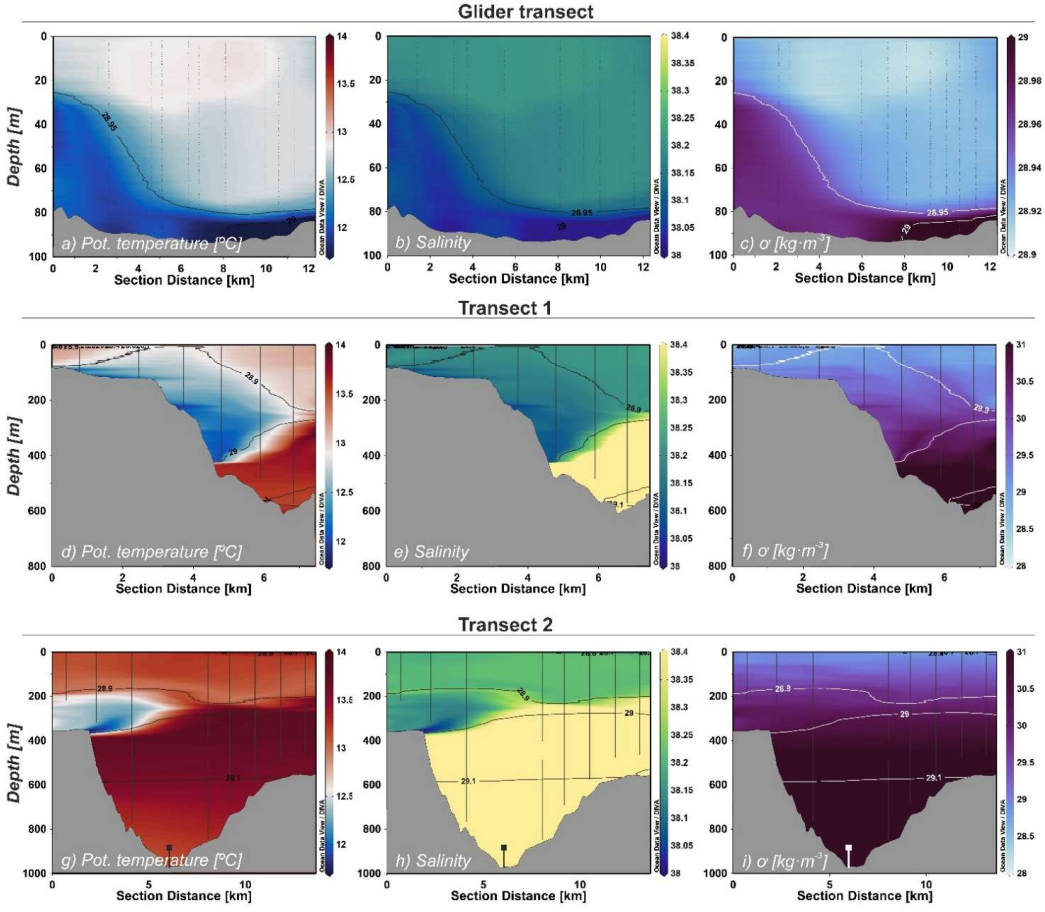

Figure 5. Contour plots of potential temperature (ºC), salinity, and potential density (σ, kg·m^{-3}) at (a-c) the continental shelf and the Cap de Creus Canyon during (d-f) T1 transect and (g-i) T2 transect. Note that for panels (a-c), the section distance goes from south to north, whereas for panels (d-i), the section distance represents a southwest-northeast direction, crossing the southern flank of the canyon. Note the change in the density scale in panel (c).

https://doi.org/10.5194/egusphere-2025-1310
Preprint. Discussion started: 28 March 2025

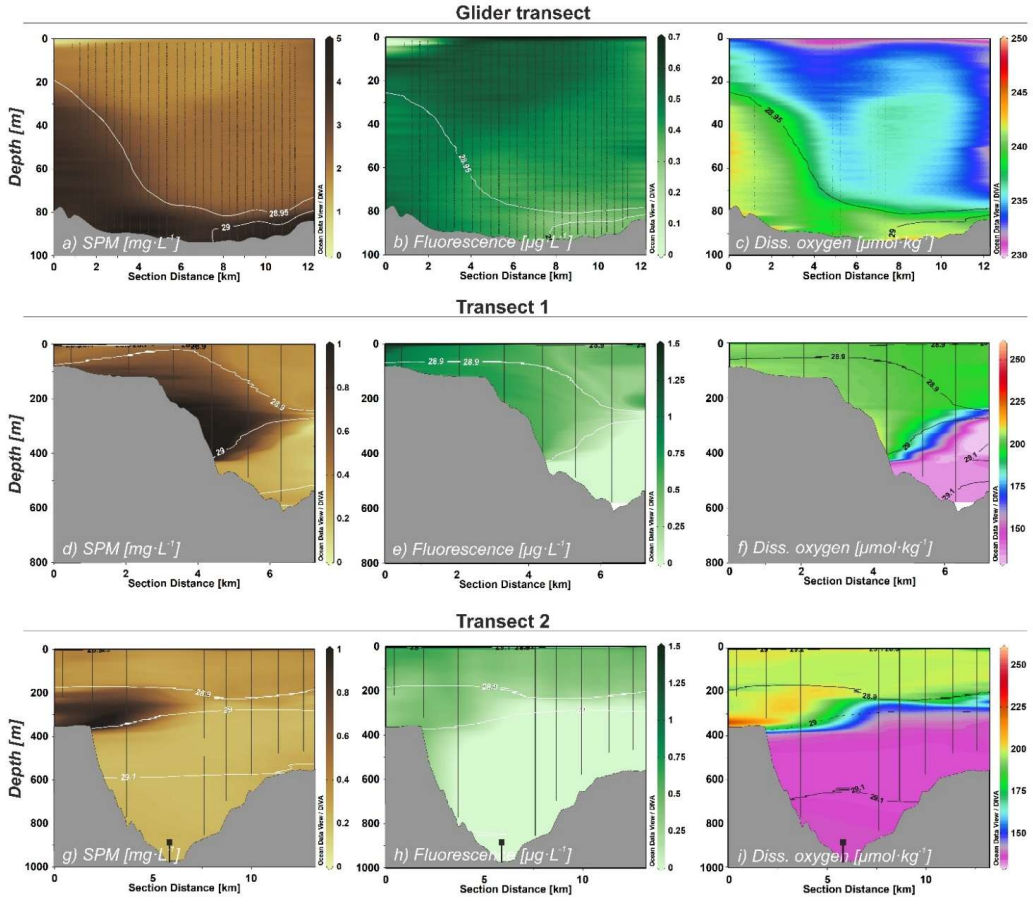

Figure 6. Contour plots of SPM concentration (mg·L^{-1}), fluorescence (µg·L^{-1}), and dissolved oxygen concentration (µmol·kg^{-1}) at (a-c) the continental shelf and at the Cap de Creus Canyon during (d-f) T1 transect and (g-i) T2 transect. Note that for panels (a-c), the section distance goes from south to north, whereas for panels (d-i) the section distance represents a southwest-northeast direction, crossing the southern flank of the canyon. Note the change in the dissolved oxygen scale in panel (c).

4.3.2 Currents

At the continental shelf, current velocity measurements indicated a fairly homogeneous current field (Figs. 7a-c). Cross-shelf currents exhibited low velocities (< 0.1 m·s^{-1}), predominantly eastward (Fig. 7a), while along-shelf currents were slightly higher (0.1-0.15 m·s^{-1}) and predominantly southward (Fig. 7b). The spatial distribution of currents averaged within the dense water vein (defined between the 28.9 and 29.0 kg·m^{-3} isopycnals) shows that dense shelf waters flowed south/south-eastward along the continental shelf adjacent to the Cap de Creus Canyon, with speeds generally around 0.15 m·s^{-1} (Fig. 7c). However, in the southern part of the section, currents were stronger, exceeding 0.2 m·s^{-1} (Fig. 7c).

In the Cap de Creus Canyon, at the T1 transect, current velocity measurements revealed the highest speeds from the surface to 400 m depth at the southern canyon flank (Figs. 7d, e). Across-canyon currents reached up to 0.3 m·s^{-1} eastward (Fig. 7d), while along-canyon currents were primarily downcanyon, with velocities between 0.1 and 0.2 m·s^{-1} (Fig. 7e). These currents appeared relatively confined within the canyon axis, with a pronounced down-canyon component (Fig. 7f). Further offshore, at the T2 transect, the highest current velocities were observed between 200 and 400 m depth (Figs. 7g, h). Across-canyon current velocities were more pronounced, and reached values of ~0.15 m·s^{-1} eastward (Fig. 7g). Along-canyon current

https://doi.org/10.5194/egusphere-2025-1310
Preprint. Discussion started: 28 March 2025

velocities were slightly smaller, ranging from 0.1 to 0.12 $m \cdot s^{-1}$ (Fig. 7h). At the southern flank, currents were weaker (~0.1 $m \cdot s^{-1}$) and predominantly southward, whereas at the northern canyon flank, these were stronger (~0.2 $m \cdot s^{-1}$) and mainly oriented towards the southeast (Fig. 7i).

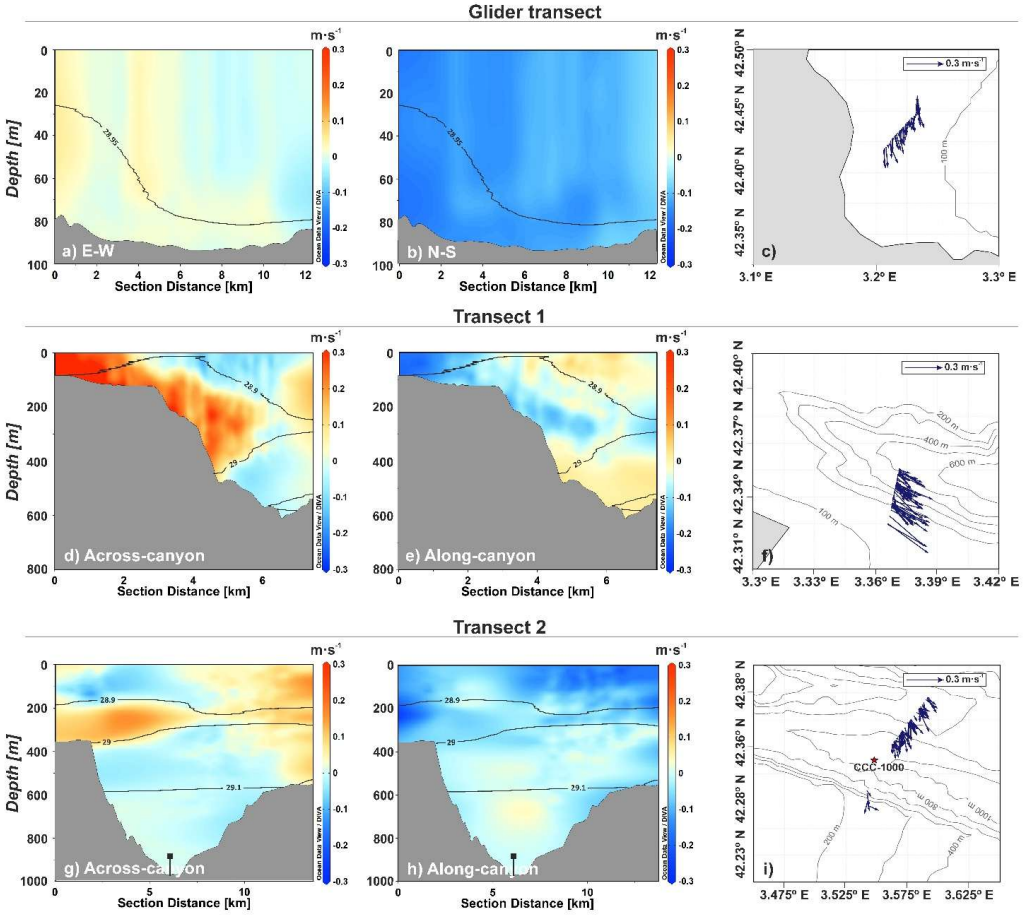

Figure 7. Contour plots of currents measured at (a-b) the continental shelf during the glider survey and at the Cap de Creus Canyon during (d-e) T1 transect and (g-h) T2 transect. In panels (a-b), eastward and northward current velocities are positive, while westward and southward current velocities are negative. Panels (d and g) represent across-canyon current velocities, while panels (e and h) represent along-canyon current velocities. Panels (c, f, and i) display stick plots representing the depth-averaged currents within the dense water vein for the three transects, defined between the 28.9 and 29.0 $kg \cdot m^{-3}$ isopycnals.

5 Discussion

5.1 Forcing conditions during winter 2021-2022

The fall-winter period 2021-2022 was characterized by a stratified water column with short northerly storms that caused continuous heat losses in the GoL and moderate river flooding (Fig. 3). During this period, seven days of easterlies/southeasterlies were recorded, similar to the winters of 2010-2011 and 2016-2017, which had 10 days (Mikolajczak et al., 2020). In contrast, the cold, dry winter of 2011-2012, a notable year for dense water formation, had only one day of easterly winds (Durrieu de Madron et al., 2013).

https://doi.org/10.5194/egusphere-2025-1310
Preprint. Discussion started: 28 March 2025

Averaged sea-atmosphere heat loss from October 2021 to early March 2022 was of -150 $W \cdot m^{-2}$ (Fig. 3a), lower than typical mild winters (-200 $W \cdot m^{-2}$) and much lower than severe winters such as 2004-2005 (-300 $W \cdot m^{-2}$) in the region (Schroeder et al., 2010). Heat loss peaked at -500 $W \cdot m^{-2}$ in November 2021 and January 2022 (Fig. 3a). This may have caused significant surface water cooling and buoyancy loss, especially on the inner shelf (Figs. 3e-g). Water temperature dropped below 12.9 ºC in late December/early January (Figs. 3e and 8a) and below 12 ºC in mid/late February (Figs. 3e and 8b). Shelf water density increased to 28.9 $kg \cdot m^{-3}$, exceeding the pre-winter maximum of 27.9 $kg \cdot m^{-3}$ (Fig. 3g). These conditions led to destratification of the water column and allowed shelf water to plunge down the slope and spread as a bottom layer across the mid and outer shelf (Figs. 3 and 8a, b). This probably marked the beginning of the cascade period, a scenario consistent with previous studies in the GoL (Dufau-Julliand et al., 2004; Durrieu de Madron et al., 2005; Canals et al., 2006; Ulses et al., 2008a).

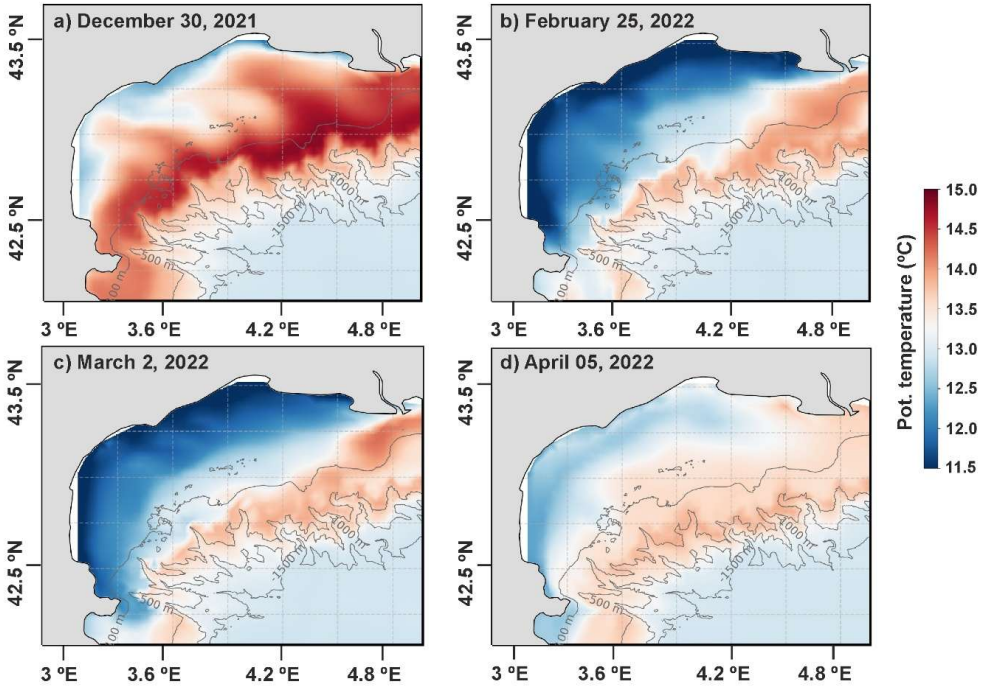

Figure 8. Bathymetric maps of the Gulf of Lion (GoL) showing the potential temperature at bottom for four days during the winter of 2021-2022: (a) December 30, 2021; (b) February 25, 2022; (c) March 2, 2022; and (d) April 5, 2022. Data has been obtained from the Mediterranean Sea Physics Reanalysis product (Escudier et al., 2020; 2021).

The cyclonic circulation on the western part of the shelf, driven by the prevailing northerly and north-westerly winds (Estournel et al., 2003), may have facilitated the transport of these dense shelf waters along the coast (Fig. 7b). The narrowing of the shelf near the Cap de Creus Peninsula further accelerated the overflow of dense shelf waters into deeper sections of the margin (Ulses et al., 2008a). However, the fresh water supplied by the rivers discharging into the GoL likely prevented a significant increase in shelf water density. During that winter, several flood events impacted the Rhône River and the smaller coastal rivers discharging into the GoL (Fig. 3d). In late December, the Rhône River discharge reached an exceptional daily value of over 5,000 $m^3 \cdot s^{-1}$ (Fig. 3d), which represents approximately three times the mean annual discharge of this river. Other moderate increases of the Rhône River discharge (> 2,000 $m^3 \cdot s^{-1}$) were recorded earlier during autumn as well as in early winter (Fig. 3d). As a result of these inputs, the salinity and density of shelf waters slightly decreased, particularly during early January (Figs. 3e, f).

https://doi.org/10.5194/egusphere-2025-1310
Preprint. Discussion started: 28 March 2025

The freshwater inputs during this period, combined with the mild meteorological conditions during winter, prevented a significant increase in the density of shelf waters (Herrman et al., 2008; Mikolajczak et al., 2020). This limitation, in turn, restricted the intrusion of dense shelf waters into deeper sections of the slope and the westernmost canyons, including the Lacaze-Duthiers and the Cap de Creus Canyons (Fig. 4g).

5.2 Advection of dense shelf waters into the Cap de Creus Canyon

During the winter 2021-2022, the density anomaly of shelf waters around 28.95 $kg \cdot m^{-3}$ was not high enough to cause cascading beyond 500 m depth (Fig. 8c). Instead, the newly formed dense shelf waters preferentially flowed southward along the coast, and only a portion was drained by the westernmost canyons (Fig. 8c). Dense shelf waters preferentially flowed into the upper and intermediate water column and did not cascade into the deeper reaches of Lacaze-Duthiers and Cap de Creus canyons. This was evidenced by the low current speeds (< 0.2 $m \cdot s^{-1}$), nearly constant temperatures (~13.5 ºC), and low SPM concentrations (< 1 $mg \cdot L^{-1}$) recorded at LDC-500, LDC-1000, and CCC-1000 mooring sites (Fig. 4). These characteristics are comparable to those reported during the mild winters of 2003-2004 (Ulses et al., 2008a) and 2010-2011 (Martín et al., 2013). In both winters, the density anomaly of shelf waters (28.8-28.9 $kg \cdot m^{-3}$) similarly limited the cascading to depths greater than 350-400 m. In contrast, during the extreme winters of 2004-2005, 2005-2006, and 2011-2012, density anomalies exceeding 29.2 $kg \cdot m^{-3}$ allowed the cascading of dense shelf waters to depths > 2,000 m, reaching the bottom of the basin (Canals et al., 2006; Font et al., 2007; Palanques et al., 2009, 2012; Durrieu de Madron et al., 2013).

In early March, the signature of dense shelf waters (T < 13 ºC and S < 38.4) was detected at the narrow continental shelf adjacent to the head of the Cap de Creus Canyon during the glider survey (Figs. 5a-c). Previous works have demonstrated that after dense water formation in the GoL, much of this water is pushed southward along the shelf by Tramontane winds and the general circulation (Ulses et al., 2008a; Bourrin et al., 2008). Once it encounters the Cap de Creus Peninsula, the dense water flow is deflected and dense shelf waters begin to pool the outer shelf until they spill into the Cap de Creus Canyon from the southern flank. This was first suggested when a large field of sedimentary furrows was found oblique to the canyon axis (Canals et al., 2006; Lastras et al., 2007), and then demonstrated through modelling by Dufau-Julliand et al. (2004) and by further observations by DeGeest et al. (2008), which found that the southern rim of the canyon is an area of sediment bypassing due to episodic strong currents during cascading events. The relatively steep bathymetry of the inner shelf, in combination with the prevailing south-eastward currents at the inner shelf (Figs. 7a-c), facilitated the transport of dense waters to the upper section of the Cap de Creus Canyon. Most likely, these dense waters were pushed into the canyon by storm-induced downwelling processes, as it was observed during the winter of 2010-2011 (Martín et al., 2013). Within the canyon, the FADWO-CCC1 T1 transect showed a vein of cold, fresher, and rich in oxygen and chlorophyll-a between 100 and 350 m depth (Figs. 5d-f and 6d-f), above the EIW found at ~500 m depth (Fig. A1). This flow traced the export of a vein of coastal dense water towards the upper continental slope, which contributed to the body of WIW (Figs. 5d-f and A1).

The WIW could have been formed earlier by DSWC events affecting the upper slope of the GoL (Lapoyade and Durrieu de Madron, 2001; Dufau-Julliand et al., 2004; Durrieu de Madron et al., 2005; Juza et al., 2019), which are especially intense between late January to early March, and then advected southward to the Cap de Creus Canyon by the general circulation. Within the Cap de Creus Canyon, the dense water vein flowed along the southern canyon flank, accompanied by increased SPM concentrations (Figs. 6 and 7). This suggests that the downwelling of dense coastal waters transported resuspended particles into the canyon down to intermediate depths (Fig. 6d). The time series of river discharge data does not seem to indicate a significant influence of the transport of sediments to the canyon (Fig. 3d). In fact, both the Rhône River and the smaller coastal rivers had low discharge before and during the FARDWO-CCC1 Cruise (Fig. 3d). This points to erosion generated by storm waves or strong currents by cascading rather than river discharge, as the main source of particles associated with the dense water vein flowing along the southern flank of the canyon. Actually, most of the sediment delivered by the GoL remains relatively close to their mouths after floods and it is later remobilized by storm waves under energetic conditions

https://doi.org/10.5194/egusphere-2025-1310
Preprint. Discussion started: 28 March 2025

(Guillén et al., 2006). Additionally, increased fluorescence values within the dense water vein (Fig. 6e) suggests the mixing of terrestrial sediments with phytoplankton cells. Phytoplankton blooms, which typically peak between December and January, likely contributed newly produced biological particles to the dense water vein, thereby enhancing the transport of organic matter into the canyon (Fig. B1; Fabres et al., 2008).

The dense water vein continued flowing down-canyon to the mid-canyon section, where it contributed to the WIW body that extended to depths of 380 m (Figs. 5g-i). At these depths, enhanced SPM concentrations were observed on the southern flank, contrasting with the clear waters on the northern canyon flank (Fig. 6g). This asymmetry has also been observed in sediment accumulation rates within the canyon, with higher rates on the northern flank and lower rates or erosion on the southern flank (DeGeest et al., 2008). These findings suggest that the southern flank acts as a bypass area during DSWC events. Southeast-flowing currents transport sediment particles along this flank, contributing to the formation of bottom and intermediate nepheloid layers (Figs. 6d, g; DeGeest et al., 2008). Meanwhile, the dense water flow within the canyon shifted from a down-canyon direction in the upper-canyon section to a more southward direction in the mid-canyon section (Figs. 7d-i). This indicates that dense waters reached their equilibrium depth. As the canyon topography opens, they are no longer confined by the canyon and began to veer towards the south, following the continental slope (Millot, 1990). Previous studies have shown that part of these dense waters can continue flowing southward, skirting the Cap de Creus Peninsula and crossing the Gulf of Roses before reaching the neighbouring Palamós Canyon (Ribó et al., 2011). Similarly, the WIW observed during the present study could have also reached the Palamós Canyon during the winter of 2021-2022, following the along-margin circulation, as previously documented in this submarine canyon during the mild winter of 2017 (February-March) (Arjona-Camas et al., 2021).

5.3 Dense shelf water export in the Cap de Creus Canyon

5.3.1 Spatial variability of the export: observational data

The total transport associated with the dense water vein in the Cap de Creus Canyon and its adjacent shelf was estimated for each CTD profile conducted during both the FARDWO-CCC1 Cruise and the glider survey in early March 2022. This estimation was based on simultaneous SPM concentration and current speed measurements. For the glider survey, SPM data were obtained from the WetLabs FLBB sensor, and current speed from the AD2CP. For the CTD transects, SPM concentrations were obtained from the SeaPoint sensor on the CTD probe, and current speed was recorded using the LADCP. Transport was integrated for each profile and across the section to estimate the total export associated with dense shelf waters. SPM transport was calculated by multiplying the estimated water transport by the SPM concentrations associated with the dense water vein. For the CTD transects, transport was calculated in vertical cells of 8 m (the bin size of the LADCP) and integrated over the different profiles across the sections. SPM concentration data were resampled to match the vertical resolution of the current speed measurements. Finally, the SPM transport was calculated using the same approach as in the glider section.

Dense shelf water transport across the continental shelf was estimated at 0.7 Sv and 10^5 metric tons from glider data. In the upper canyon section (T1 transect), the total transport associated with the dense water flow was 0.3 Sv, including 10^5 tons of suspended particulate matter. At the mid-canyon section (T2), transport decreased to 0.05 Sv, with roughly 10^4 metric tons of suspended particulate matter. These values are comparable to those observed during the mild winter of 2010-2011 in the Cap de Creus Canyon (Martín et al., 2013). The transport decrease between T1 and T2 suggests that most dense water flow remained on the shelf and shelf edge around the Cap de Creus Canyon Peninsula, rather than fully cascading into the canyon. This indicates that during mild winters, the Cap de Creus Canyon acts only as a partial sink for cascading waters.

https://doi.org/10.5194/egusphere-2025-1310
Preprint. Discussion started: 28 March 2025

5.3.2 Temporal variability of the export: reanalysis data

The MedSea reanalysis product was used to assess the variability of dense shelf water export in the Cap de Creus Canyon during the mild winter of 2021-2022. This analysis focused on estimating the temporal variability of dense water export along the canyon two cross-sections near the T1 and T2 transects (Fig. 9a). Daily reanalysis data on seawater potential temperature and eastward velocities were used to calculate the transport of dense waters at intermediate depths across these sections during autumn, winter, and early spring. The results indicated that export was generally higher in winter, with transport magnitudes being higher in the upper canyon section compared to the mid-canyon section (Figs. 9b, c). Similar to our observational data, these results suggest that dense waters did not penetrate deeply into the canyon but remained on the shelf and around the canyon head.

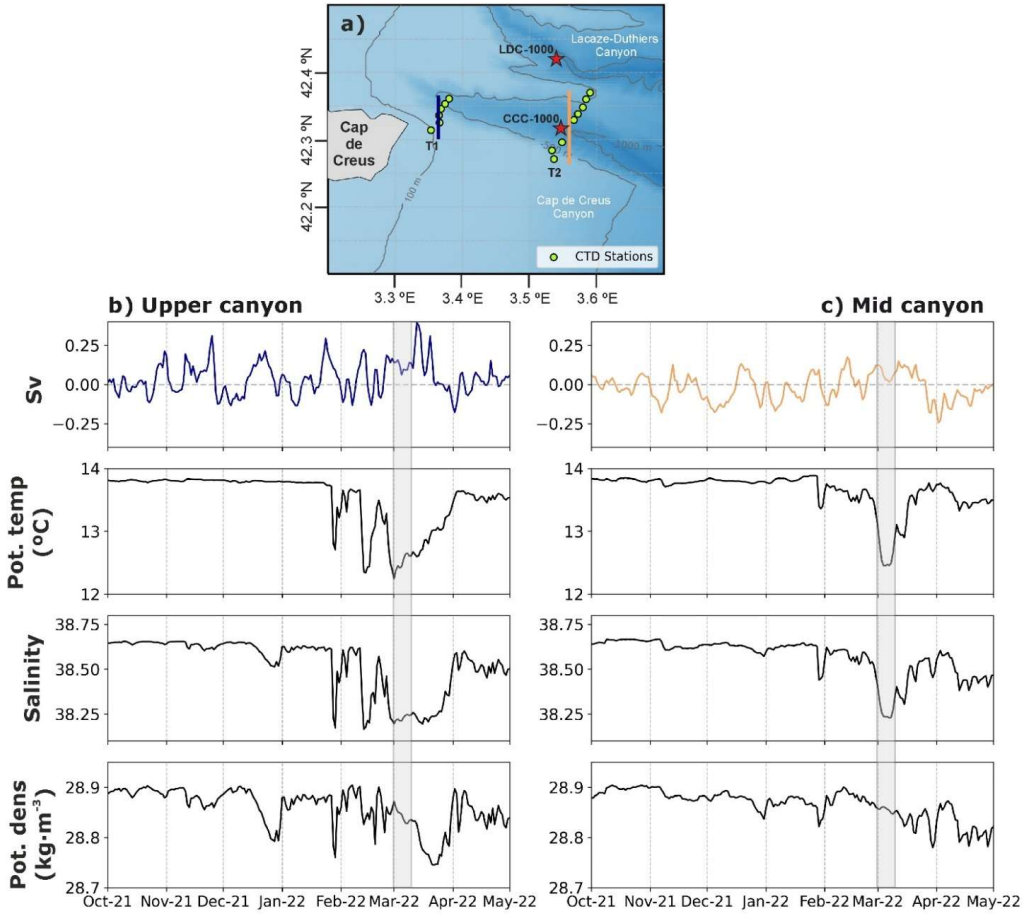

Figure 9. (a) Bathymetric map showing the location of T1 and T2 transects (green dots) conducted during the FARDWO-CCC1 Cruise (March 2022). The two transects used to estimate the temporal variability of the along-canyon transport at intermediate depths (350 m depth), located near T1 and T2, are also shown as coloured lines; (b-c) Time series of along-canyon transport of dense waters (in Sv) and its associated thermohaline characteristics (potential temperature, salinity, and potential density) for two transects: (b) the upper-canyon transect (blue line, near T1) and (c) the mid-canyon section (orange line, near T2), extracted from the Mediterranean Sea Physics Reanalysis product (Escudier et al., 2020; 2021). Positive values in the first panels indicate down-canyon transport, while negative values indicate up-canyon transport.

https://doi.org/10.5194/egusphere-2025-1310
Preprint. Discussion started: 28 March 2025

Moreover, seasonal variability in dense water transport was strongly influenced by meteorological and hydrological conditions (Fig. 3). During autumn, the GoL experienced multiple northerly and northwesterly windstorms (lasting between 1 to 3 consecutive days), along with maximum heat losses that contributed to the cooling and densification of shelf waters (Fig. 3). In early November 2021, the Rhône River discharged 2,492 $m^3 \cdot s^{-1}$ of freshwater into the GoL (Fig. 3d). The arrival of this coastal freshwater in the upper canyon section was evident in the reanalysis time series, marked by a slight decrease in salinity and potential density (Fig. 9b).

Winter experienced longer periods of moderate northerly and northwesterly winds (blowing between 5 to 7 consecutive days) and higher discharge from the Rhône River (Fig. 3d). By late December, another significant discharge event from the Rhône River reached the upper canyon section (Fig. 3d), again leading to decreased salinity and potential density (Fig. 9a). The enhanced freshwater input, in addition to wind forcing, likely helped to inhibit the densification of shelf waters over the GoL, preventing their transport into deeper sections of the Cap de Creus Canyon. Notably, no significant temperature increase was observed in the reanalysis time series during this period (Fig. 9b). A significant increase in dense water export occurred in late January, coinciding with the arrival of cold ($T < 12.9$ ºC) and relatively dense waters in the canyon (Fig. 9b). This signal was also detected in the mid-canyon section, although with lower transport magnitude (Fig. 9c), suggesting the onset of the cascading period in the canyon. Two additional cascading pulses were also identified in mid-February and late-March, both associated with an increase in down-canyon transport (Fig. 9b). The increased transport export in March, particularly in the upper-canyon section (Fig. 9b), and to a lesser extent in the mid-canyon section (Fig. 9c), followed a period of easterly-southeasterly winds (Fig. 3b), which most likely triggered or intensified the export within the canyon. The role of marine storms has previously been documented during other mild winters, such as 2003-2004 and 2010-2011, when marine storms played a key role in driving downwelling processes (Ulses et al., 2008a; Rumín-Caparrós et al., 2013).

As spring progressed, neat heat losses gradually decreased (Fig. 3a), likely due to rising atmospheric temperatures. This led to a gradual decline in dense water export, which ceased by early April (Fig. 9a). Accordingly, the duration of the cascading period in the Cap de Creus Canyon, defined as the period between the first and last cascading event (Palanques et al., 2006), was approximately three months, from January to early April 2022 (Figs. 8d and 9).

5.4 Impact of climate change on DSWC dynamics

Our estimates indicate that during the mild winter of 2021-2022, approximately 40 % of the dense shelf water export occurred through the Cap de Creus Canyon, primarily within its upper section, while the remaining 60 % was transported along the coast. This distribution contrasts with the extreme, cold winter of 2004-2005, when nearly 70 % of the export took place through the canyon (Ulses et al., 2008b). These findings suggest that during mild events, DSWC may primarily influence coastal ecosystems, whereas in extreme winters, when dense waters reach deeper areas, DSWC can significantly impact deep-sea habitats (Mikolajczak et al., 2020).

Future climate projections indicate an increasing frequency of mild winters in the northwestern Mediterranean (Herrmann et al., 2008; Durrieu de Madron et al., 2023). Under the IPCC-A2 scenario, DSWC could decline by 90 % at the end of the 21st century (Herrmann et al., 2008). This scenario would drastically reduce both the intensity and depth penetration of DSWC. A recent study by Margirier et al. (2020) has already pointed out a warming and salinification of surface and intermediate waters across the northwestern Mediterranean basin, which would increase stratification and hinder deep-ocean convection. Such reduction in deep DSWC could strengthen the production of WIW by favouring intermediate-water formation over deep-water ventilation (Parras-Berrocal et al., 2022). Consequently, dense shelf water transport may become more limited to near-coastal areas rather than cascading into deeper areas of the continental slope, thus altering the regional hydrology and impacting the Mediterranean Thermohaline Circulation (Somot et al., 2006). Ongoing sea warming and increasing stratification in the water column could further alter shelf-slope exchanges, reducing DSWC and the associated transport of particulate matter from the GoL to the deep basin (Somot et al., 2006). As a result, the transfer of shelf waters and organic

https://doi.org/10.5194/egusphere-2025-1310
Preprint. Discussion started: 28 March 2025

matter to the deep sea could be drastically reduced and mainly redirected along the Catalan shelf. The reduction of deep DSWC would not only reorient the main export routes of dense shelf waters but could also have far-reaching consequences for deep-sea ecosystems. Cold water corals, benthic organisms, and commercially important species (such as shrimps) may be particularly affected, as the limited supply of nutrients and oxygen would hinder their survival (Pusceddu et al., 2013).

Additionally, the weakening of DSWC could significantly alter sediment transport pathways, affecting erosion and deposition patterns along the incised submarine canyons of the GoL. Changes in sediment dynamics could impact benthic communities that rely on the arrival of suspended particulate matter. For example, Puig et al. (2001) suggested that slope intermediate nepheloid layers, loaded with fine particulate matter rich in organic matter, play a significant role in the settlement of the larvae of benthic species to the seabed, turning nepheloid layers into prime nursery habitats. Regardless of the direction of DSWC's effects on deep-sea ecosystems, it has been demonstrated that even a minor loss of biodiversity can result in major ecosystem collapse (Danovaro et al., 2008), with predictable impacts on ecosystem services, including fisheries (Pörtner and Knust, 2007; Smith et al., 2009).

6 Conclusions

This study used a multiplatform approach, combining data from gliders, ship-based CTD transects, instrumented mooring lines, and reanalysis products to assess dense-shelf water and associated sediment transport in the Cap de Creus Canyon during the mild winter of 2021-2022. The winter of 2021-2022 was characterized by several days of northerly and north-westerly windstorms that induced sustained heat losses in the GoL region, enhancing the formation of dense shelf waters. Nevertheless, the moderate freshwater inputs from the Rhône River and the smaller coastal rivers decreased the density of shelf waters and, consequently, limited their export into deeper sections of Lacaze-Duthiers and Cap de Creus Canyons.

In early March 2022, dense shelf waters were observed in the glider transect conducted at the continental shelf adjacent to the Cap de Creus Canyon. They were transported to the upper canyon section to depths of ~350 m, where they contributed to the formation of the WIW. Increased SPM concentrations were also observed at the same water depths, likely indicative of a resuspension process. River discharges were low before and during the FARDWO-CCC1 cruise and, therefore, they were not the main source of suspended sediments during the downwelling phase. Erosion induced by the action of storm waves or strong currents by cascading waters were likely the main contributor of suspended sediments associated with the dense water vein transported through the canyon. We estimated a roughly dense water transport of ~0.3 Sv and 10^5 metric tons of sediments on the upper canyon section. Late winter was marked by persistent northerly and northwesterly windstorms alternated with easterly-southeasterly wind events, which reinforced the presence and flushing of dense shelf waters into the Cap de Creus Canyon.

Reanalysis data provided additional temporal context, revealing that the cascading season lasted approximately three months, from January to early April 2022. This data also showed multiple shallow cascading pulses during this period, with the peak export in late-January and mid-March, highlighting the episodic nature of DSWC. This data also showed that much of the dense water export took place along the coast, while only a small portion downwelled into the westernmost canyons incising the GoL (namely Lacaze-Duthiers and Cap de Creus canyons) between 200 and 400 m depth.

Future investigations should aim to expand observational datasets, not only within the westernmost canyons incising the gulf but also across the shelf areas. Increasing glider surveys on the GoL's shelf area could improve our understanding of dense water export during weak cascading events under mild winter conditions. Further investigations should also focus on the changes in WIW. These studies would help to understand the alterations in the water column properties and changes in stratification affecting convection processes, which directly impact the Mediterranean circulation and the climate system.

https://doi.org/10.5194/egusphere-2025-1310
Preprint. Discussion started: 28 March 2025

Data availability

The data that support the findings of this study are publicly available under the following links: SeaExplorer glider from (https://data-selection.odatis-ocean.fr/coriolis/uri/p83112098), CCC-1000 moored time series (https://doi.org/10.17882/104746; Sanchez-Vidal et al., 2025a), LDC-500 and LDC-1000 moored time series (https://doi.org/10.17882/45980; Durrieu de Madron et al., 2024). The CTD and the ADCP data collected during the FARDWO-CCC1 Cruise are available at https://doi.org/10.17882/105499 (Sanchez-Vidal et al., 2025b).

Author contributions

AS, DA, XD, and FB defined the research problem, the conceptualization of the study, and leaded the acquisition of the study data. MA-C carried out the data analysis and produced the figures and first draft of the manuscript. All coauthors discussed the analyses and contributed to the review and writing of the final paper.

Competing interests

The authors declare that they have no conflict of interest.

Acknowledgements

We are very grateful to the captain, crew, and the scientific team for their dedication and hard work during the FARDWO-CCC1 Cruise at the R/V *García del Cid*, and to the technicians for their guidance and assistance. We wish to thank the Alseamar Alcen technicians for the glider deployment and piloting, and the data pre-processing. We also want to thank Pascal Conan from OSU-Stamar (Stations Marines UPMC de Banyuls-sur-Mer) at the Sorbonne Université, as well as acknowledge the MOOSE, the COAST-HF and the SOMLIT programs coordinated by CNRS-INSU and the Research Infrastructure ILICO (CNRS-IFREMER) for providing data from the POEM and SOLA buoys and the Lacaze-Duthiers Canyon's mooring.

Financial support

This work has been supported by the FAR-DWO (PID2020-114322RB-I00) project funded by MICIU/AEI/10.13039/501100011033, the Catalan Government Excellent Research Groups grant no. 2021 SGR 01195, and the ANR MELANGE (ANR-19-ASMA-0004) project. MAC is supported by a Margarita Salas postdoctoral grant from the Spanish Ministry of Universities.

References

Arjona-Camas, M., Puig, P., Palanques, A., Durán, R., White, M., Paradis, S., and Emelianov, M.:. Natural vs. trawling-induced water turbidity and suspended sediment transport variability within the Palamós Canyon (NW Mediterranean). Mar. Geophys. Res. 42, 38, https://doi.org/10.1007/s11001-021-09457-7, 2021.

Béthoux, J., Durrieu de Madron, X., Nyffeler, F., and Taiiliez, D.: Deep water in the western Mediterranean: peculiar 1999 and 2000 characteristics, shelf formation hypothesis, variability since 1970 and geochemical interferences. J. Mar. Sys. 33, 117-131, http://doi.org/ 10.1016/S0924-7963(02)00055-6, 2002.

Blair, N. E., and Aller, R. C.: The fate of terrestrial organic carbon in the marine environment. Annu. Rev. Mar. Sci. 4, 401-423, https://doi.org/10.1146/annurev-marine-120709-142717, 2012.

https://doi.org/10.5194/egusphere-2025-1310
Preprint. Discussion started: 28 March 2025

Bourrin, F. and Durrieu de Madron, X.: Contribution to the study of coastal rivers and associated prodeltas to sediment supply in the Gulf of Lions (NW Mediterranean Sea). Life Environ. 56, 307-31, 2006.

Bourrin, F., Durrieu de Madron, X., Heussner, S., and Estournel, C. : Impact of winter dense water formation on shelf sediment erosion (evidence from the Gulf of Lions, NW Mediterranean). Cont. Shelf Res. 28, 1984-1999, https://doi.org/10.1016/j.csr.2008.06.006, 2008.

Bourrin, F., Many, G., Durrieu de Madron, X., Martín, J., Puig, P., Houpert, L., Testor, P., Kunesch, S., Mahiouz, K., and Béguery, L.: Glider monitoring of shelf suspended particle dynamics and transport during storm and flooding conditions. Cont. Shelf Res. 109, 135-149, https://doi.org/10.1016/j.csr.2015.08.031, 2015.

Bourrin, F., Zudaire, L., Vala, T., Vuillemin, R., Conan, P., and Kunesch, S. : POEM Coastal Buoy. SEANOE. https://doi.org/10.17882/88936, 2022.

Canals, M., Puig, P., Durrieu de Madron, X., Heussner, S., Palanques, A., and Fabres, J.: Flushing submarine canyons. Nature d444, 354-357, https://doi.org/10.1038/nature05271, 2006.

Conan, P., Maria, E., Labatut, P., Zudaire, L., Pujo-Pay, M., Pecqueur, D., Salmeron, C., Crispi, O., Marie, B., and Vuillemin, R.: SOMLIT-SOLA time series (French Research Infrastructure ILICO): long-term core parameter monitoring in the Bay of Banyuls-sur-Mer. SEANOE. https://doi.org/10.17882/99794, 2024.

Danovaro, R., Gambi, C., Dell'Anno, A., Corinaldesi, C., Fraschetti, S., Vanreusel, A., Vincx, M., and Gooday, A. : Exponential decline of deep-sea ecosystem functioning linked to benthic ecosystem loss. Curr. Biol. 18, 1-18, https://doi.org/10.1016/j.cub.2007.11.056, 2008.

Davis, R. A., and Hayes, M. O. : What is a wave-dominated coast ? Mar. Geol. 60, 313-319, https://doi.org/10.1016/0025-3227(84)90155-5, 1984.

DeGeest, A.L., Mullenbach, B. L., Puig, P., Nittrouer, C. A., Drexler, T. M., Durrieu de Madron, X., Orange, D. L. : Sediment accumulation in the western Gulf of Lions, France : the role of Cap de Creus Canyon in linking shelf and slope sediment dispersal systems. Cont. Shelf Res. 28, 2031-2047, https://doi.org/10.1016/j.csr.2008.02.008, 2008.

Dipper, F. : The seawater environment and ecological adaptations, in : Elements of Marine Ecology (Fifth Edition), edited by : Butterworth-Heinemann, Oxford, UK, 37-151, https://doi.org/10.1016/B978-0-08-102826-1.00002-8, 2022.

Drexler, T. M., and Nittrouer, C. A.: Stratigraphic signatures due to flood deposition near the Rhône River: Gulf of Lions, northwest Mediterranean Sea. Cont. Shelf Res. 28, 1877-1894, https://doi.org/10.1016/j.csr.2007.11.012, 2008.

Dufau-Julliand, C., Marsaleix, P., Petrenko, A., and Dekeyser, I.: Three-dimensional modeling of the Gulf of Lion's hydrodynamics (northwest Mediterranean) during January 1999 (MOOGLI3 Experiment) and late winter 1999: Western Mediterranean Intermediate Water's (WIW's) formation and its cascading over the shelf break. J. Geophys. Res. Oceans, 109, https://doi.org/10.1029/2003JC002019, 2004.

Durrieu de Madron, X., Nyffeler, F., and Godet, C. H. : Hydrographic structure and nepheloid spatial distribution in the Gulf of Lions continental margin. Cont. Shelf Res. 10, 915-929, https://doi.org/10.1016/0278-4343(90)90067-V, 1990.

Durrieu de Madron, X. and Panouse, M. : Transport de matière en suspension sur le plateau continental du Golfe de Lion-Situation estivale et hivernale. Comptes Rendus de l'Académie des Sciences, Série IIa, Paris, 322, 1061-1070, 1996.

Durrieu de Madron, X., Zervakis, V., Therocharis, A., and Georgopoulos, D.: Comments on "Cascades of dense water around the world ocean". Prog. Oceanogr. 64, 83-90, https://doi.org/10.1016/j.pocean.2004.08.004, 2005.

Durrieu de Madron, X., Wiberg, P. L., and Puig, P. Sediment dynamics in the Gulf of Lions: The impact of extreme events. Cont. Shelf Res. 28, 1867-1876, https://doi.org/10.1016/j.csr.2008.08.001, 2008.

Durrieu de Madron, X., Houpert, L., Puig, P., Sanchez-Vidal, A., Testor, P., Bosse, A., Estournel, C., Somot, S., Bourrin, F., Bouin, M. N., Beauverger, M., Beguery, L., Canals, M., Cassou, C., Coppola, L., Dausse, F., D'Ortenzio, F., Font, J., Heussner, S., Kunesch, S., Lefevre, D., Le Goff, H., Martín, J., Mortier, L., Palanques, A., and Raimbault, P.: Interaction

https://doi.org/10.5194/egusphere-2025-1310
Preprint. Discussion started: 28 March 2025

of dense shelf water cascading and open-sea convection in the northwestern Mediterranean during winter 2012. Geophys. Res. Lett. 40, 1379-1385, https://doi.org/10.1002/grl.50331, 2013.

Durrieu de Madron, X., Aubert, D., Charrière, B., Kunesch, S., Menniti, C., Radakovitch, O., and Sola, J.: Impact of dense water formation on the transfer of particles and trace metals from the coast to the deep in the northwestern Mediterranean. Water, 15, 301, https://doi.org/10.3390/w15020301, 2023.

Durrieu de Madron, X., Heussner, S., Delsaut, N., Stéphane, K., Menniti, C.: BILLION observatory data. SEANOE. https://doi.org/10.17882/45980, 2024.

Escudier, R., Clementi, E., Omar, M., Cipollone, A., Pistoia, J., Aydogdu, A., Drudi, M., Grandi, A., Lyubartsev, V., Lecci, R., Cretí, S., Masina, S., Coppini, G., and Pinardi, N.: Mediterranean Sea Physical Reanalysis (CMEMS MED-Currents) (Version 1) [Data set]. Copernicus Monitoring Environment Marine Service (CMEMS), https://doi.org/10.25423/CMCC/MEDSEA_MULTIYEAR_PHY_006_004_E3R1, 2020.

Escudier, R., Clementi, E., Cipollone, A., Pistoia, J., Drudi, M., Grandi, A., Luybartsev, V., Lecci, R., Aydogdu, A., Delrosso, D., Omar, M., Masina, S., Coppini, G., and Pinardi, N.: A high resolution reanalysis for the Mediterranean Sea. Front. Earth Sci. 9, 702285, https://doi.org/10.3389/feart.2021.702285, 2021.

Estournel, C., Durrieu de Madron, X., Marsaleix, P., Auclair, F., Julliand, C., and Vehil, R. : Observation and modeling of the winter coastal oceanic circulation in the Gulf of Lion under wind conditions influenced by the continental orography (FETCH experiment). J. Geophys. Res. Oceans, 108, https://doi.org/10.1029/2001JC000825, 2003.

Estournel, C., Mikolajczak, G., Ulses, C., Bourrin, F., Canals, M., Charmasson, S., Doxaran, D., Duhaut, T., Durrieu de Madron, D., Marsaleix, P., Palanques, A., Puig, P., Radakovitch, O., Sanchez-Vidal, A., and Verney, R. : Sediment dynamics in the Gulf of Lion (NW Mediterranean Sea) during two autumn–winter periods with contrasting meteorological conditions. Prog. Oceanogr. 210, 102942, https://doi.org/10.1016/j.pocean.2022.102942, 2023.

Fabres, J., Tesi, T., Velez, J., Batista, F., Lee, C., Calafat, A., Heussner, S., Palanques, A., and Miserocchi, S. : Seasonal and event-controlled export of organic matter from the shelf towards the Gulf of Lions continental slope. Cont. Shelf Res. 28, 1971-1983, https://doi.org/10.1016/j.csr.2008.04.010, 2008.

Feistel, R.: A new extended Gibbs thermodynamic potential of seawater. Prog. Oceanogr. 58, 43-114, https://doi.org/10.1016/S0079-6611(03)00088-0, 2003.

Feistel, R.: A Gibbs function for seawater thermodynamics for -6 to 80 C and salinity up to 120 $g \cdot kg^{-1}$. Deep Sea Res. I Oceans, 55, 1639-1671, https://doi.org/10.1016/j.dsr.2008.07.004, 2008.

Ferré, B., Durrieu de Madron, X., Estournel, C., Ulses, C., and Le Corre, G. : Impact of natural (waves and currents) and anthropogenic (trawl) resuspension on the export of particulate matter to the open ocean: application to the Gulf of Lion (NW Mediterranean). Cont. Shelf Res. 28, 2071-2091, https://doi.org/10.1016/j.csr.2008.02.002, 2008.

Fischer, J., and Visbeck, M.: Deep Velocity Profiling with Self-contained ADCPs. J. Atmos. Ocean. Technol. 10, 764-773, https://doi.org/10.1175/1520-0426(1993)010%3C0764:DVPWSC%3E2.0.CO;2, 1993.

Font, J.: The path of the Levantine intermediate water to the Alboran Sea. Deep Sea Res. I Oceanogr. Res. Pap. 34, 1745-1755, https://doi.org/10.1016/0198-0149(87)90022-7, 1987.

Font, J., Puig, P., Salat, J., Palanques, A., and Emelianov, M.: Sequence of hydrographic changes in the NW Mediterranean deep water due to the exceptional winter of 2005. Sci. Mar. 71, 339-346, https://doi.org/10.3989/scimar.2007.71n2339, 2007.

Fugate, D.C., and Friedrichs, C.T.: Determining concentration and fall velocity of estuarine particle populations using ADV, OBS and LISST. Cont. Shelf Res. 22 (11–13), 1867–1886, https://doi.org/10.1016/S0278-4343(02)00043-2, 2002.

Gartner, J. W.: Estimating suspended soils concentrations from backscatter intensity measured by acoustic Doppler current profiler in San Francisco Bay, California. Mar. Geol. 211, 169-187, https://doi.org/10.1016/j.margeo.2004.07.001, 2004.

https://doi.org/10.5194/egusphere-2025-1310
Preprint. Discussion started: 28 March 2025

Guillén, J., Bourrin, F., Palanques, A., Durrieu de Madron, X., Puig, P., and Buscail, R.: Sediment dynamics during 735 'wet' and 'dry' storm events on the Têt inner shelf (SW Gulf of Lions). Mar. Geol. 234, 129-142, https://doi.org/10.1016/j.margeo.2006.09.018, 2006.

Guizien, H.: Spatial variability of wave conditions in the Gulf of Lions (NW Mediterranean Sea). Vie et Milieu/Life & Environment, 261-270, 2009.

Herrmann, M., Estournel, C., Déqué, M., Marsaleix, P., Sevault, F., and Somot, S. : Dense water formation in the 740 Gulf of Lions shelf: Impact of atmospheric interannual variability and climate change. Cont. Shelf Res. 28, 2092-2112, https://doi.org/10.1016/j.csr.2008.03.003, 2008.

Hersbach, H., Bell, B., Berrisford, P., Biavati, G., Horányi, A., Muñoz Sabater, J., Nicolas, J., Peubey, C., Radu, R., Rozum, I., Schepers, D., Simmons, A., Soci, C., Dee, D., and Thépaut, J-N. ERA5 hourly data on pressure levels from 1940 to present. Copernicus Climate Change Service (C3S) Climate Data Store (CDS). https://doi.org/10.24381/cds.bd0915c6, 745 2024.

Heussner, S., Durrieu de Madron, X., Calafat, A., Canals, M., Carbonne, J., Desault, N., and Saragoni, G.: Spatial and temporal variability of downward particle fluxes on a continental slope: lessons from an 8-yr experiment in the Gulf of Lions (NW Mediterranean). Mar. Geol. 234, 63-92, https://doi.org/10.1016/j.margeo.2006.09.003, 2006.

Homrani, S., de Fommervault, P., Gentil, M., Jourdin, F., Durrieu de Madron, X., Bourrin, F. : Tracing suspended 750 sediment fluxes using a glider : observations in a tidal shelf environment. EGUsphere, 1-35, https://doi.org/10.5194/egusphere-2024-4072, 2025.

Houpert, L., Durrieu de Madron, X., Testor, P., Bosse, A., D'Ortenzio, F., Bouin, M. N., Dausse, D., Le Goff, H., Kunesch, S., Labaste, M., Coppola, L., Mortier, L., and Raimbault, P. : Observations of open-ocean deep convection in the northwestern Mediterranean Sea: Seasonal and interannual variability of mixing and deep water masses for the 2007-2013 755 Period. J. Geophys. Res. Oceans, 121, 8139-8171, https://doi.org/10.1002/2016JC011857, 2016.

Kwon, E., DeVries, T., Galbraith, E. D., Hwang, J., Kim, G., and Timmermann, A.: Stable carbon isotopes suggest large terrestrial carbon inputs to the global ocean. Global Biogeochem. Cycles 35: e2020GB006684, https://doi.org/10.1029/2020GB006684, 2021.

Juza, M., Renault, L., Ruiz, S., and Tintoré, J.: Origin and pathways of Winter Intermediate Water in the Northwestern 760 Mediterranean Sea using observations and numerical simulation. J. Geophys. Res. 118, 6621-6633, https://doi.org/10.1002/2013JC009231, 2013.

Juza, M., Escudier, R., Vargas-Yáñwz, M., Mourre, B., Heslop, E., Allen, J., and Tintoré, J.: Characterization of changes in Western Intermediate Water properties enabled by an innovative geometry-based detection approach. J. Mar. Sys. 191, 1-12, https://doi.org/10.1016/j.jmarsys.2018.11.003, 2019.

765 Lastras, G., Canals, M., Urgeles, R., Amblas, D., Ivanov, M., Droz, L., Dennielou, B., Fabrés, J., Schoolmeester, T., Akhmetzhanov, A., Orange, D., and García-García, A.: A walk down the Cap de Creus Canyon, Northwestern Mediterranean Sea: Recent processes inferred from morphology and sediment bedforms. Mar. Geol. 246, 176-192, https://doi.org/10.1016/j.margeo.2007.09.002, 2007.

Lapouyade A. and Durrieu de Madron, X. : Seasonal variability of the advective transport of particulate and organic 770 carbon in the Gulf of Lion (NW Mediterranean). Oceanol. Acta, 24, 295-312, https://doi.org/10.1016/S0399-1784(01)01148-3, 2001.

Le Bot, P., Kermabon, C., Lherminier, P., and Gaillard, F.: CASCADE V6.1: Logiciel de validation et de visualisation des mesures ADCP de coque. Rapport technique OPS/LPO 11-01. Ifremer, Centre de Brest, France, 2011.

Leredde, Y., Denamiel, C., Brambilla, E., Lauer-Leredde, C., Bouchette, F., and Marsaleix, P. : Hydodynamics in the 775 Gulf of Aigues-Mortes, NW Mediterranean Sea: In situ and modelling data. Cont. Shelf Res. 27, 2389-2406, https://doi.org/10.1016/j.csr.2007.06.006, 2007.

https://doi.org/10.5194/egusphere-2025-1310
Preprint. Discussion started: 28 March 2025

Levin, L. A. and Sibuet, M.: Understanding continental margin biodiversity: a new imperative. Annu. Rev. Mar. Sci. 4, 79-112, http://doi.org/10.1146/annurev-marine-120709-142714, 2012.

Liu, Z., Zhao, Y., Colin, C., Stattegger, K., Wiesner, M. G., Huh, C. A., Zhang, Y., Li, X., Sompongchaiyakul, P., You, C. F., Huany, C., Liu, J. T., Siringan, F. P., Le, Sathiamurthy, E., Hantoro, W. S., Liu, J., Tuo, S., Zhao, S., Zhou, S., He, Z., Wang, Y., Bunsomboonsakul, S., and Li, Y.: Source-to-sink transport processes of fluvial sediments in the South China Sea. Earth Sci. Rev. 153, 238-273, https://doi.org/10.1016/j.earscirev.2015.08.005, 2016.

Lohrmann, A.: Monitoring Sediment Concentration with Acoustic Backscattering Instruments. Nortek, 2001.

Ludwig, W., Dumont, E., Meybeck, M., and Heussner, S.: River discharges of water and nutrients to the Mediterranean and Black Sea: major drivers for ecosystem changes during past and future decades? Prog. Oceanogr. 80, 199-217, https://doi.org/10.1016/j.pocean.2009.02.001, 2009.

Margirier, F., Testor, P., Heslop, E., Mallil, K., Bosse, A., Houpert, L., Mortier, L., Bouin, M., Coppola, L., D'Ortenzio, F., Durrieu de Madron, X., Mourre, B., Prieur, L., Raimbault, P., and Taillandier, V. : Abrupt warming and salinification of intermediate waters interplays with decline of deep convection in the Northwestern Mediterranean Sea. Sci. Rep. 10, 20923, https://doi.org/10.1038/s41598-020-77859-5, 2020.

Martín, J., Durrieu de Madron, X., Puig, P., Bourrin, F., Palanques, A., Houpert, L., Higueras, M., Sánchez-Vidal, A., Calafat, A. M., Canals, M., Heussner, S., Delsaut, N., and Sotin, C. : Sediment transport along the Cap de Creus canyon flank during a mild, wet winter. Biogeosciences 10(5):3221-3239, https://doi.org/10.5194/bg-10-3221-2013, 2013.

Marshall, J., and Schott, F.: Open-ocean convection: Observations, theory, and models. Rev. Geophys. 37, 1-64, https://doi.org/10.1029/98RG02739, 1999.

Mendoza, E. T. and Jiménez, A. A.: Vulnerability assessment to coastal storms at a regional scale. In: Coastal engineering 2008, vol. 5, pp. 4154-4166, https://doi.org/10.1142/9789814277426_0345, 2009.

Mikolajczak, G., Estournel, C., Ulses, C., Marsaleix, P., Bourrin, F., Martín, J., Pairaud, I., Puig, P., Leredde, Y., Many, G., Seyfried, L., and Durrieu de Madron, X.: Impact of storms on residence times and export of coastal waters during a mild autumn/winter period in the Gulf of Lion. Cont. Shelf Res. 207, 104192, https://doi.org/10.1016/j.csr.2020.104192, 2020.

Millot, C.: The Gulf of Lions' hydrodynamics. Cont. Shelf Res. 10, 885-894, https://doi.org/10.1016/0278-4343(90)90065-T, 1990.

Millot, C.: Circulation in the Western Mediterranean. J. Mar. Syst. 20, 423-442, https://doi.org/10.1016/S0924-7963(98)00078-5, 1999.

Nittrouer, C. A., Austin, J. A., Field, M. E., Kravitz, J. H., Syvitski, J. P., and Wiberg, P. L.: Continental margin sedimentation: from sediment transport to sequence stratigraphy, John Wiley and Sons (Eds), http://doi.org/10.1002/9781444304398, 2009.

Odic, R., Bensoussan, N., Pinazo, C., Taupier-Letage, I., and Rossi, V. : Sporadic wind-driven upwelling/downwelling and associated cooling/warming along Northwestern Mediterranean coastlines. Cont. Shelf Res. 250, 104843, https://doi.org/10.1016/j.csr.2022.104843, 2022.

Ogston, A. S., Drexler, T. M., and Puig, P.: Sediment delivery, resuspension, and transport in two contrasting canyon environments in the southwest Gulf of Lions. Cont. Shelf Res. 28, 2000-2016, https://doi.org/10.1016/j.csr.2008.02.012, 2008.

Palanques, A., Durrieu de Madron, X., Puig, P., Fabrés, J., Guillén, J., Calafat, A., Canals, M., Heussner, S., and Bonnin, J.: Suspended sediment fluxes in the Gulf of Lions submarine canyons. The role of storms and dense water cascading. Mar. Geol. 234, 43-61, https://doi.org/10.1016/j.margeo.2006.09.002, 2006.

Palanques, A., Guillén, J., Puig, P., and Durrieu de Madron, X.: Storm-driven shelf-to-canyon suspended sediment transport at the southwestern Gulf of Lions. Cont. Shelf Res. 28, 1947-1956, https://doi.org/10.1016/j.csr.2008.03.020, 2008.

https://doi.org/10.5194/egusphere-2025-1310
Preprint. Discussion started: 28 March 2025

Palanques, A., Puig, P., Latasa, M., and Scharek, R.: Deep sediment transport induced by storms and dense shelf-water cascading in the northwestern Mediterranean basin. Deep Sea Res. Pt I. 56, 425-434, https://doi.org/10.1016/j.dsr.2008.11.002, 2009.

Palanques, A., Puig, P., Durrieu de Madron, X., Sanchez-Vidal, A., Pasqual, C., Martín, J., Calafat, A., Heussner, S., and Canals, M. : Sediment transport to the deep canyons and open-slope of the western Gulf of Lions during the 2006 intense cascading and open-sea convection period. Prog. Oceanogr. 106, 1-15, https://doi.org/10.1016/j.pocean.2012.05.002, 2012.

Palanques, A., and Puig, P.: Particle fluxes induced by benthic storms during the 2012 dense shelf water cascading and open sea convection period in the northwestern Mediterranean Basin. Mar. Geol. 406, 119-131, https://doi.org/10.1016/j.margeo.2018.09.010, 2018.

Parras-Berrocal, I. M., Vázquez, R., Cabos, W., Sein, D. V., Álvarez, O., Bruno, M., and Izquierdo, A.: Surface and intermediate water changes triggering the future collapse of deep water formation in the North Western Mediterranean. Geophys. Res. Lett. 49, e2021GL095404, https://doi.org/10.1029/2021GL095404, 2022.

Pasqual, C., Sanchez-Vidal, A., Zúñiga, D., Calafat, A., Canals, M., Durrieu de Madron, X., Puig, P., Palanques, A., and Delsaut, N.: Flux and composition of settling particles across the continental margin of the Gulf of Lion: the role of dense shelf water cascading. Biogeosciences, 7, 217-231, https://doi.org/10.5194/bg-7-217-2010, 2010.

Petrenko, A.: Variability of circulation features in the Gulf of Lion, NW Mediterranean Sea. Importance of inertial currents. Oceanol. Acta 26: 323–338, https://doi.org/10.1016/S0399-1784(03)00038-0, 2008.

Petrenko, A., Dufau, C., and Estournel, C.: Barotropic eastward currents in the western Gulf of Lion, north-western Mediterranean Sea, during stratified conditions. J. Mar. Syst. 74, 406-428, https://doi.org/10.1016/j.jmarsys.2008.03.004, 2008.

Pont, D., Simonnet, J. P., and Walter, A. V.: Medium-term changes in suspended sediment delivery to the ocean: consequences of catchment heterogeneity and river management (Rhône River, France). Estuar. Coast. Shelf Sci. 54, 1-18, http://doi.org/10.1006/ecss.2001.0829, 2002.

Pörtner, H. O. and Knust, R.: Climate change affects marine fishes through oxygen limitation of thermal tolerance. Science, 315, 95-97, https://doi.org/10.1126/science.1135471, 2007.

Poulier, G., Launay, M., Le Bescond, C., Thollet, F., Coquery, M., and Le Coz, J.: Combining flux monitoring and data reconstruction to establish annual budgets of suspended particulate matter, mercury and PCB in the Rhône River from Lake Geneva to the Mediterranean Sea. Sci. Total Environ. 658, 457-273, https://doi.org/10.1016/j.scitotenv.2018.12.075, 2019.

Puig, P., Company, J. B., Sardà, F., and Palanques, P. : Responses of deep-water shrimp populations to intermediate nepheloid layer detachments on the Northwestern Mediterranean continental margin. Deep Sea Res. I Oceanogr. Res. Pap. 48, 2195-2207, https://doi.org/10.1016/S0967-0637(01)00016-4, 2001.

Puig, P., Palanques, A., Orange, D. L., Lastras, G., and Canals, M.: Dense shelf water cascades and sedimentary furrow formation in the Cap de Creus Canyon, northwestern Mediterranean Sea. Cont. Shelf Res. 28, 2017-2030, https://doi.org/10.1016/j.csr.2008.05.002, 2008.

Puig, P., Palanques, A., and Martín, J.: Contemporary sediment-transport in submarine canyons. Annu. Rev. Mar. Sci. 6, 53-77, https://doi.org/10.1146/annurev-marine-010213-135037, 2014.

Pusceddu, A., Mea, M., Canals, M., Heussner, S., Durrieu de Madron, X., Sanchez-Vidal, A., Bianchelli, S., Corinaldesi, A., Dell'Anno, A., Thomsen, L., and Danovaro, R.: Major consequences of an intense dense shelf water cascading event on deep-sea benthic trophic conditions and meiofaunal biodiversity. Biogeosciences 10, 2659-2670, https://doi.org/10.5194/bg-10-2659-2013, 2013.

https://doi.org/10.5194/egusphere-2025-1310
Preprint. Discussion started: 28 March 2025

Raimbault, P., and Durrieu de Madron, X.: Research activities in the Gulf of Lion (NW Mediterranean) within the 1997-2001 PNEC Project. Oceanol. Acta 26, 291-298, https://doi.org/10.1016/S0399-1784(03)00030-6, 2003.

Ribó, M., Puig, P., Palanques, A., and Lo Iacono, C.: Dense shelf water cascades in the Cap de Creus and Palamós submarine canyons during winters 2007 and 2008. Mar. Geol. 284, 175-188, https://doi.org/10.1016/j.margeo.2011.04.001, 2011.

Rumín-Caparrós, A., Sanchez-Vidal, A., Calafat, A. M., Canals, M., Martín, J., Puig, P., and Pedrosa-Pàmies, R.: External forcings, oceanographic processes and particle flux dynamics in Cap de Creus submarine canyon, NW Mediterranean. Biogeosciences Discussions 9(12), https://digital.csic.es/handle/10261/78113, 2013.

Sadaoui, M., Ludwig, W., Bourrin, F., and Raimbault, P.: Controls, Budgets and Variability of Riverine Sediment Fluxes to the Gulf of Lions (NW Mediterranean Sea). J. Hydrol. 540, 1002–1015, https://doi.org/10.1016/j.jhydrol.2016.07.012, 2016.

Sanchez-Vidal, A., Pasqual, C., Kerhervé, P., Heussner, S., Palanques, A., Durrieu de Madron, X., Canals, M., and Puig, P.: Impact of dense shelf water cascading on the transfer of organic matter to the deep western Mediterranean basin. Geophys. Res. Lett. 35, https://doi.org/10.1029/2007GL032825, 2008.

Sanchez-Vidal, A., Calafat, A., Amblas, D., Cerdà-Domènech, M., Fos, H.: CC1000 observatory data. SEANOE. https://doi.org/10.17882/105504, 2025a.

Sanchez-Vidal, A., Amblas, D., Arjona-Camas, M., Durrieu de Madron, X., Calafat, A., Cerdà-Domènech, M., Pena, L.D., Espinosa, S.: CTD and ADCP data collected during the cruise FARDWO CC1. SEANOE. http://doi.org/10.17882/105499, 2025b.

Schroeder, K., Josey, S. A., Herrmann, M., Grignon, L., Gasparini, G. P., and Bryden, H. L.: Abrupt warming and salting of the Western Mediterranean Deep Water: Atmospheric forcings and lateral advection. J. Geophys. Res., 115, C08029, https://doi.org/10.1029/2009JC005749, 2010.

Schroeder, K., Ben Ismail, S., Bensi, M., Bosse, A., Chiggiato, K., Civitarese, G., Falcieri M, F., Fusco, G., Gacic, M., Gertman, I., Kubin, E., Malanotte-Rizzoli, P., Martellucci, R., Menna, M., Ozer, T., Taupier-Letage, I., Vargas-Yañez, M., Velaoras, D. and Vilibic, I.: A consensus-based, revised and comprehensive catalogue for Mediterranean water masses acronyms. *Mediterranean Marine Science*, *25*(3), 783–791, https://doi.org/10.12681/mms.38736, 2024.

Serrat, P., Ludwig, W., Navarro, B., and Blazi, J. L.: Variabilité spatio-temporelle des flux de matières en suspension d'un fleuve côtier méditerranéen: la Têt (France). Comptes Rendus de l'Académie des Sciences-Series IIA-Earth and Planetary Science, 333(7), 389-397, https://doi.org/10.1016/S1251-8050(01)01652-4, 2001.

Smith, M. D., Knapp, A. K., and Collins, S. L. : A framework for assessing ecosystem dynamics in response to chronic resource alterations induced by global change. Ecology, 90, 3279-3289, https://doi.org/10.1890/08-1815.1, 2009.

Somot, S., Sevault, F., and Déqué, M. : Transient climate change scenario simulation of the Mediterranean Sea for the twenty-first century using a high-resolution ocean circulation model. Clim. Dynam. 27, 851-879, https://doi.org/10.1007/s00382-006-0167-z, 2006.

Somot, S., Houpert, L., Sevault, F., Testor, P., Bosse, A., Taupier-Letage, I., Bouin, M. N., Waldman, R., Cassou, C., Sanchez-Gomez, E., Durrieu de Madron, X., Adloff, F., Nabat, P., and Herrmann, M.: Characterizing, modelling and understanding the climate variability of the deep water formation in the North-Western Mediterranean Sea. Clim. Dynam. 51, 1179-1210, https://doi.org/10.1007/s00382-016-3295-0, 2016.

Taillandier, V., D'Ortenzio, F., Prieur, L., Conan, P., Coppola, L., Cornec, M., Dumas, F., Durrieu de Madron, X., Fach, B., Fourrier, M., Gentil, M., Hayes, D., and Husrevoglu, S.: Sources of the Levantine Intermediate Water in winter 2019. J. Geophys. Res. Oceans, 127, e2021JC017506, https://doi.org/10.1029/2021JC017506, 2022.

Tesi, T., Puig, P., Palanques, A., and Goñi, M.: Lateral advection of organic matter in cascading-dominated submarine canyons. Prog. Oceanogr. 84, 185-203, https://doi.org/10.1016/j.pocean.2009.10.004, 2010.

https://doi.org/10.5194/egusphere-2025-1310
Preprint. Discussion started: 28 March 2025

Testor, P., Bosse, A., Houpert, L., Margirier, F., Mortier, L., Le Goff, H., Dausse, D., Labaste, M., Kartensen, J., Hayes, D., Olita, A., Ribotti, A., Schroeder, K., Chiggiato, J., Onken, R., Heslop, E., Mourre, B., D'Ortenzio, F., Mayot, N., Lavigne, H., Durrieu de Madron, X., Bourrin, F., Many, G., Damien, P., Estournel, C., Marsaleix, P., Taupier-Letage, I., Raimbault, P., Waldman, R., Bouin, M. N., Giordani, H., Caniaux, G., Somot, S., Ducrocq, V., and Conan, P.: Multiscale observations of deep convection in the northwestern Mediterranean Sea during winter 2012-2013 using multiple platforms. J. Geophys. Res. Oceans, 123, 1745-1776, https://doi.org/10.1002/2016JC012671, 2018.

Thurnherr, A. M., Symonds, D., and Laurent, L. S.: Processing explorer ADCP data collected on slocum gliders using the LADCP shear method. In Proceedings of the 2015 IEEEOES 11th Current Waves and Turbulence Measurement CWTM. St. Petersburg, FL, USA 2-6 March 2015, https://doi.org/10.1109/CWTM.2015.7098134, 2015.

Ulses, C., Estournel, C., Bonnin, J., Durrieu de Madron, X., and Marsaleix, P. : Impact of storms and dense water cascading on shelf-slope exchanges in the Gulf of Lion (NW Mediterranean). J. Geophys. Res. Oceans, 113, http://doi.org/10.1029/2006JC003795, 2008a.

Ulses, C., Estournel, C., Puig, P., Durrieu de Madron, X., and Marsaleix, P.: Dense shelf water cascading in the northwestern Mediterranean during the cold winter 2005: Quantification of the export through the Gulf of Lion and the Catalan margin. Geophys. Res. Lett. 35(7), https://doi.org/10.1029/2008GL033257, 2008b.

Visbeck, M.: Deep velocity profiling using lowered acoustic Doppler current profilers: Bottom track and inverse solutions. J. Atmos. Oceanic Technol. 19, 794-807, https://doi.org/10.1175/1520-0426(2002)019%3C0794:DVPULA%3E2.0.CO;2, 2002.

Walsh, J. P., and Nittrouer, C. A.: Understanding fine-grained river-sediment dispersal on continental margins. Mar. Geol. 263, 34-45, https://doi.org/10.1016/j.margeo.2009.03.016, 2009.

Wilson, G. W., and Hay, A. E.: Acoustic backscatter inversion for suspended sediment concentration and size: a new approach using statistical inverse theory. Cont. Shelf Res. 106, 130-139, https://doi.org/10.1016/j.csr.2015.07.005, 2015.

https://doi.org/10.5194/egusphere-2025-1310
Preprint. Discussion started: 28 March 2025

Appendix A – Hydrographic data collected during the FARDWO-CCC1 cruise in the Cap de Creus Canyon and the glider survey on the adjacent continental shelf during March 2022.

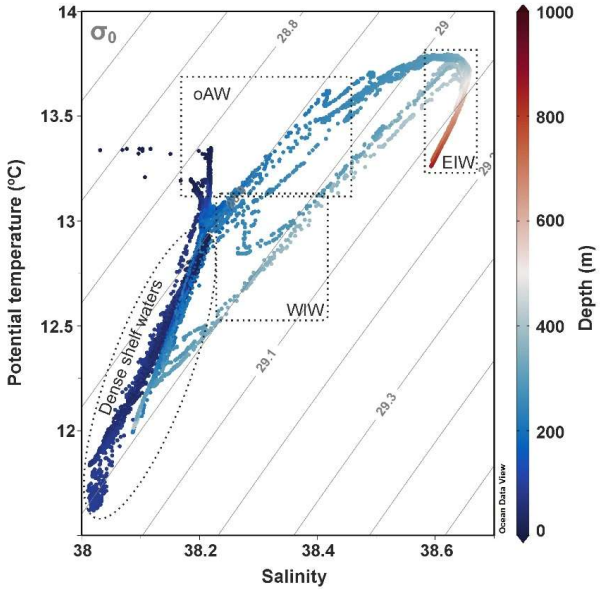

Figure A1. *TS* diagram from the CTD profiles collected during FARDWO-CCC1 T1 and T2 transects across the Cap de Creus Canyon, as well as those collected during the glider survey at the adjacent shelf (see Fig. 1b for positions). The different water masses that can be identified in the study area are: dense shelf waters, oAW (old Atlantic Water), WIW (Western Intermediate Water), and EIW (Eastern Intermediate Water).

https://doi.org/10.5194/egusphere-2025-1310
Preprint. Discussion started: 28 March 2025

Appendix B – Seasonality of chlorophyll-a between October 2021 and April 2022 from in situ measurements at the SOLA station.

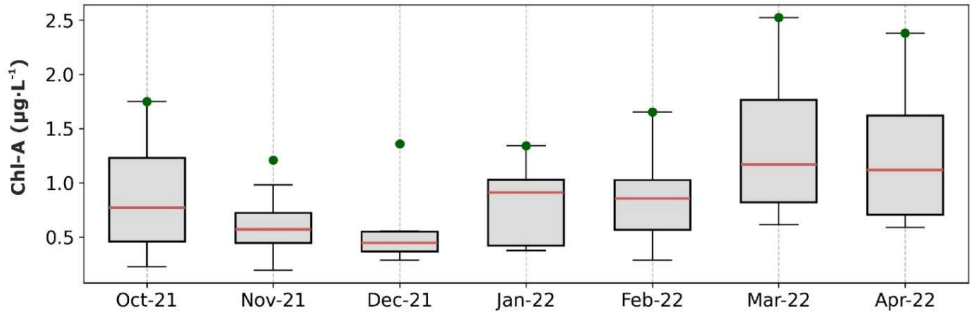

Figure B1. Seasonality of the chlorophyll-a measured at SOLA station between October 2021 and April 2022. Green dots indicate the monthly maximum values. Data has been retrieved from the SOMLIT-SOLA monitoring site in the Bay of Banyuls-sur-Mer (https://www.seanoe.org/data/00886/99794/; Conan et al., 2024).